รายงานการวิจัยฉบับสมบูรณ์

การเร่งปฏิกิริยาเพื่อเปลี่ยนกลีเซอรอลให้เป็นแอลกอฮอล์

Catalytic Conversion of Glycerol to Alcohols

รศ.ดร.ตะวัน สุขน้อย

ดร.ณัฐธิดา นุ่มวงศ์

ได้รับทุนสนับสนุนงานวิจัยจากงบประมาณเงินรายได้ ประจำปีงบประมาณ พ.ศ.2559

คณะวิทยาศาสตร์

สถาบันเทคโนโลยีพระจอมเกล้าเจ้าคุณทหารลาดกระบัง

ชื่อโครงการ การเร่งปฏิกิริยาเพื่อเปลี่ยนกลีเซอรอลให้เป็นแอลกอฮอล์
แหล่งเงิน งบประมาณเงินรายได้
ประจำปีงบประมาณ 2559 จำนวนเงินที่ได้รับการสนับสนุน 300,000 บาท
ระยะเวลาทำการวิจัย 1 ปี ตั้งแต่ 1 ตุลาคม 2558 - 30 กันยายน 2559
หัวหน้าโครงการวิจัย รศ.ดร.ตะวัน สุขน้อย ภาควิชาเคมี คณะวิทยาศาสตร์
ผู้ร่วมโครงการวิจัย ดร.ณัฐธิดา นุ่มวงศ์ ภาควิชาเคมี คณะวิทยาศาสตร์

บทคัดย่อ

กลีเซอรอลเป็นผลิตภัณฑ์ข้างเคียง ที่ได้จากการผลิตไบโอดีเซลจึงน่าสนใจเป็นอย่างยิ่ง ดังนั้น การวิจัย และพัฒนาเทคโนโลยีกระบวนการ เพื่อเพิ่มมูลค่าให้กับกลีเซอรอล ในงานวิจัยนี้ได้ศึกษาการเปลี่ยนกลีเซอรอลไปเป็น 1-โพราพานอล ในระบบเบดต่อเนื่อง ซึ่งในเบดบนนั้น ใช้ซีโอไลต์ H-ZSM-5 เป็นตัวเร่งปฏิกิริยา สำหรับการขจัดน้ำออกจากโมเลกุลของกลีเซอรอล ได้อะโครลีน เป็นผลิตภัณฑ์หลักถึงร้อยละ 80 และไฮดรอกซีอะซีโตนเป็นผลิตภัณฑ์รองร้อยละ 15 และในเบดล่าง ใช้ตัวเร่งปฏิกิริยา 20% นิเกิล บนตัวรองรับชนิดต่างๆ ซิลิกา อะลูมินา ไทเทเนียมออกไซด์ ถ่านกัมมันต์ แมกนีเซียมออกไซด์ เลเยอร์ดับเบิลไฮดรอกไซด์ เพื่อทำปฏิกิริยาการเติมไฮโดรเจน จากผลการทดลองปรากฏว่า โพรพานาล-ดีไฮด์ เป็นสารมัธยันต์ที่จะเปลี่ยนเป็น 1-โพรพานอล ผ่านปฏิกิริยาการเติมไฮโดรเจน นอกจากนี้ โพรพานาลดีไฮด์ ยังสามารถทำปฏิกิริยากับน้ำได้เป็นกรดโพรพาโนอิก และยิ่งไปกว่านั้น อันตรกิริยาระหว่างโลหะกับตัวรองรับชนิดต่างๆ ยังส่งผลให้ตัวเร่งปฏิกิริยามีประสิทธิภาพที่แตกต่างกันด้วย ซึ่งความสามารถในการเติมไฮโดรเจนของตัวเร่งปฏิกิริยา เรียงลำดับดังนี้ นิกเกิล บนตัวรองรับอะลูมินา > บนไทเทเนียมออกไซด์ > บนเลเยอร์ดับเบิลไฮดรอกไซด์ > บนซิลิกา > บนแมกนีเซียมออกไซด์ > บนถ่านกัมมันต์ และอุณหภูมิในช่วง 120-200 องศาเซลเซียส เป็นช่วงที่เหมาะสมสำหรับปฏิกิริยาการเติมไฮโดรเจนของอะโครลีน แต่อย่างไรก็ตาม พบการเสื่อมสภาพของตัวเร่งปฏิกิริยา จากการฝังตัวของผลิตภัณฑ์ที่มีโมเลกุลขนาดใหญ่ ปรากฏให้เห็นในงานวิจัยนี้ด้วย

คำสำคัญ : กลีเซอรอล นิเกิล ปฏิกิริยาการเติมไฮโดรเจน 1-โพรพานอล

Research Title: Catalytic Conversion of Glycerol to Alcohols

Researcher: Assoc. Prof. Dr. Tawan Sooknoi

Dr. Natthida Numwong

Faculty: Science Department: Chemistry

ABSTRACT

Glycerol is a low-value by-product from the biodiesel process. The conversion of glycerol to more valuable products is of such interest. In this research, the deoxygenation of glycerol to 1-propanol in sequential bed system was studied. In the upper bed, H-ZSM-5 (Si/Al ratio 12.5) was used as a catalyst for the dehydration of glycerol. From that first system, acrolein is a major product and hydroxyacetone is a minor product with the yield of 80% and 15%, respectively. In the lower bed, 20 wt.% Ni on various supports (Ni/Al_2O_3, Ni/SiO_2, Ni/TiO_2, Ni/LDH, Ni/MgO, and Ni/C) were used for the hydrogenation reaction of acrolein. The results suggest that propionaldehyde is an intermediate which further yield the desired 1-propanol via hydrogenation. Moreover, this compound could also react with water yielding propanoic acid. In addition, the interaction between metal on various supports demonstrates the different catalytic performances. The hydrogenation activities of the catalyst are in the order of: Ni/Al_2O_3 > Ni/TiO_2 > Ni/LDH > Ni/SiO_2 > Ni/MgO > Ni/C. The reaction temperature in the range of 120-200^{o}C is suitable for promoting the acrolein hydrogenation. However, the catalytic deactivation was observed due to the deposition of high molecular product over the catalyst.

Keywords : glycerol, nickel, hydrogenation, 1-propanol

กิตติกรรมประกาศ

ขอขอบคุณสมาชิกกลุ่มวิจัย Catalytic Chemistry Research Unit และเจ้าหน้าที่ นักวิทยาศาสตร์ ประจำภาควิชาเคมี คณะวิทยาศาสตร์ ทุกท่านที่ให้การช่วยเหลือในการวิจัยครั้งนี้ เป็นอย่างดี

การวิจัยครั้งนี้ได้รับทุนสนับสนุนการวิจัยจากสถาบันเทคโนโลยีพระจอมเกล้าเจ้าคุณทหารลาดกระบัง จากงบประมาณเงินรายได้ ประจำปีงบประมาณ พ.ศ.2559

รศ.ดร.ตะวัน สุขน้อย

ดร.ณัฐธิดา นุ่มวงศ์

สารบัญ

หน้า

สารบัญ (ต่อ)

หน้า

สารบัญ (ต่อ)

หน้า

สารบัญตาราง

ตารางที่ **หน้า**

สารบัญภาพ

ภาพที่ **หน้า**

สารบัญภาพ (ต่อ)

ภาพที่ **หน้า**

บทที่ 1

บทนำ

1.1 ความเป็นมาและความสำคัญของปัญหา

Nowadays, the demand of petroleum fuel and energy usage increases steadily due to an expansion of economy; while, the source of fossil fuel depletes steadily. Therefore, alternative energy is required to replace petroleum fuel. One of the examples is biodiesel produced from renewable sources, such as palm oil. Biodiesel production process via transesterification reaction produces glycerol, which is a valuable by-product. Glycerol is widely used as a raw material to augment value of chemical compounds, for example, 1,2-propanediol, acrolein, and hydroxyacetone. Glycerol molecule composes of three hydroxyl groups. In order to extend the use of glycerol, the hydroxyl groups should be removed [1]. Dehydration of glycerol over acid catalysts produces acrolein and various by-products. Acrolein is an unsaturated aldehyde, a suitable substrate for converting into other high value chemical compounds, such as 1-propanol.

The conversion of glycerol to 1-propanol proceeds via dehydration-hydrogenation. Dehydration yields acrolein as a main product, followed by hydrogenation to 1-propanol, in which propionaldehyde is an intermediate. Acidic catalysts, such as alumina or zeolite, can be used for dehydrating glycerol to acrolein [2,3]. Among the acid catalysts, H-ZSM-5 possesses the high surface area as well as acidity and acid strength. The hydrogenation of acrolein formed can be promoted by active metal catalysts, such as palladium, silver, nickel, and platinum over various inert supports, such as silica and activated carbon [4]. Nickel is typically used as a catalyst for hydrogenation because it is common and relatively cheaper than palladium and platinum. In general, acrolein is highly reactive that can be converted to other products during dehydration process and also difficult to handle for the storage. Accordingly, the conversion of acrolein to more stable product will be occurred immediately after its formation. In addition, acrolein facilitate high selectivity to alcohols via hydrogenation at the C=C bond. This hydrogenation reaction can take place in the gas-

phase over transitions metal catalysts, such as platinum, palladium, and nickel. This leads to the formation of propionaldehyde and consequently 1-propanol.

In this study, the conversion of glycerol to 1-propanol is investigated in a continuous fixed-bed reactor using sequential bed system. Acid H-ZSM-5 catalyst is used in the upper bed; while, supported nickel catalysts were used in the lower bed. From the previous study [2], the reaction conditions in the first catalytic bed were fixed at 300oC, 1 atm, and contact time of 1.7 mmol/h. The effect of contact time, reaction temperature and catalyst support in the second catalytic bed on the activity and selectivity towards 1-propanol is investigated in this research.

1.2 วัตถุประสงค์ของโครงการวิจัย

1. To produce 1-propanol from glycerol using sequential bed system (H-ZSM-5 and supported Ni catalysts)

2. To understand the effect of reaction temperature, contact time, and catalyst support on the activity and selectivity of the catalyst in the second bed

3. To understand the mechanism of the conversion of glycerol to 1-propanol

4. To explain deactivation behavior of the catalyst

1.3 ขอบเขตของโครงการวิจัย

The scopes of this special project are as follows:

1. Preparation of the hydrogenation bed by wetness impregnation: 20 wt.% nickel on silica (SiO_2), **γ**-alumina (**γ**-Al_2O_3), activated carbon, titanium dioxide (TiO_2), magnesium oxide (MgO) and layered double hydroxides (LDH) supports

2. Characterization of the prepared catalyst by X-ray Diffractometer (XRD), X-ray Fluorescence (XRF), Temperature Programmed Reduction (TPR), Temperature Programmed

Desorption (TPD), Gas adsorption analysis (BET), Transmission electron microscopy (TEM) and Thermal gravimetric analysis (TGA)

3. Study on reaction temperature in a range of 100-200°C with contact time between 15-177 g.h/mol to evaluate the catalytic activity and selectivity in a continuous fixed-bed system of those reaction conditions

4. Analysis of liquid products by Gas Chromatography with Flame Ionization Detector (GC-FID)

1.4 วิธีดำเนินการวิจัย

1. Catalyst Preparation and modification

1.1 Preparation of H-ZSM-5 Support

1.2 Preparation of 20 wt.% Ni supported silica (SiO2), **γ**-alumina (**γ**-Al2O3), titanium dioxide (TiO_2), magnesium dioxide (MgO) and layered double hydroxides (LDH) catalysts.

1.3 Preparation of 20 wt.% Ni supported activated carbon catalyst (Ni/C)

2. Characterization of catalysts

2.1 X-ray diffraction (XRD)

2.2 X-ray fluorescence (XRF)

2.3 N_2-Gas adsorption analysis

2.4 Temperature programmed reduction (TPR)

2.5 Temperature programmed desorption (TPD)

2.6 Transmission electron microscopy (TEM)

2.7 Thermal gravimetric analysis (TGA)

3. Catalytic Activity testing

3.1 Dehydration of glycerol to acrolein

3.2 Subsequent hydrogenation of glycerol dehydrated products

4. Products analysis

1.5 ประโยชน์ที่คาดว่าจะได้รับ

It is expected that a new technology for producing 1-propanol from glycerol will be obtained and developed with higher efficiency.

บทที่2

ทฤษฎีและงานวิจัยที่เกี่ยวข้อง

2.1 ทฤษฎีที่เกี่ยวข้อง

2.1.1 Glycerol

Glycerol information

Glycerol shown in Figure 2.1 is a chemical, which has a multitude of uses in pharmaceutical, cosmetic, and food industries. Glycerol produced from oleochemical or biodiesel plant is usually in a crude form that contains various impurities, such as oily, alkali, soap components, and a salt or diols, depending on the processes and the type of materials processed [1,5]. Crude glycerol is a low value product as its low purity limits its application as feedstock in industries.

Properties of glycerol

Glycerol is an organic compound with the chemical formula of $C_3H_8O_3$. It is synonymous to glycerin, propane-1,2,3-triol, 1,2,3-propanetriol, 1,2,3-trihydroxypropane, glyceritol, and glycyl alcohol. Glycerol has a low toxicity alcohol that consists of three-carbon chains with a hydroxyl group attached to each carbon (Figure 2.1) that is virtually nontoxic to both human and environment [5].

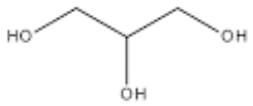

Figure 2.1 Structure of glycerol

Physically, glycerol is a clear, colorless, odorless, hygroscopic, vicious, and sweet taste liquid. The boiling point, melting point and flash point of glycerol is 290°C, 18°C, and 177°C, respectively [6]. Under normal atmospheric pressure, glycerol has a molecular weight of 92.09 g/mol, a density of 1.261 g/cm^3, and a viscosity of 1.5 Pa.s [7].

Glycerol is a good solvent for many substances, such as iodine, bromine and phenol due to the presence of the hydroxyl group. Glycerol is chemically stable under normal storage and handling conditions; nevertheless, it may become explosive when it is in contact with strong oxidizing agents, such as potassium chlorate [8]

Source of glycerol

Glycerol can be generated from transesterification of fat and oils in biodiesel plant. Transesterification is a chemical reaction, whereby, fat and oils (triglycerides) react with alcohol, for example, methanol in the presence of a catalyst to produce fatty acid methyl esters with glycerol as a byproduct, as presented in Figure 2.2.

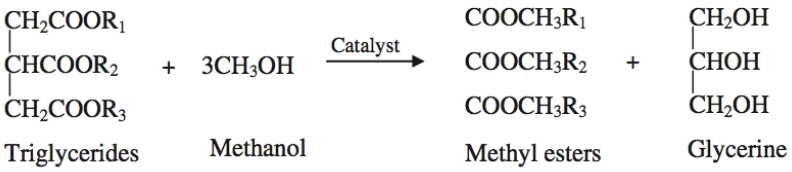

Figure 2.2 Transesterification reaction

Glycerol to higher valuable products

Glycerol is a valuable by-product as it has a wide range of industrial applications. At present, glycerol has over two thousand different applications [9], especially in pharmaceuticals, personal care, foods, and cosmetics, as shown in Figure 2.3. Glycerol is a nontoxic, edible, biodegradable compound; thus, it provides important environmental benefits to the new platform products.

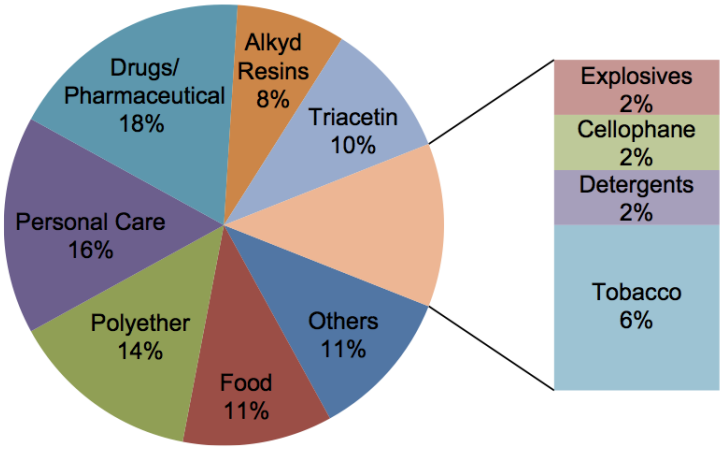

Figure 2.3 Glycerol industrial applications [10]

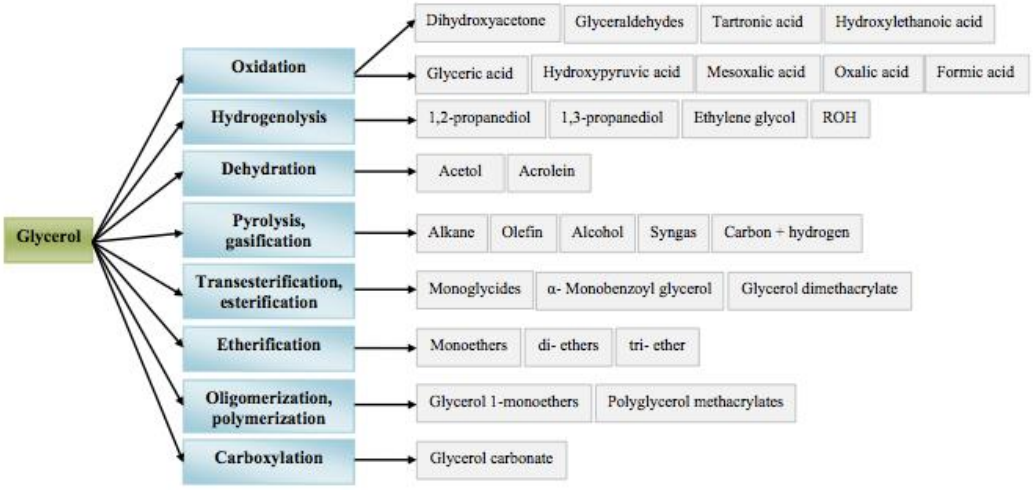

Figure 2.4 Glycerol conversion methodologies for the production of different higher valuable chemicals [11]

Dehydration of Glycerol

Dehydration reaction usually proceeds in aqueous media with the continuous extraction. Strong acids, such as ion-exchange resins and zeolites, have been used as catalysts for this reaction. There are several advantages of using zeolites. Firstly, zeolites are selective catalysts because side reactions and C-C cleavage are less important [12]. Moreover, they are regenerated easily and can be operated at high temperature. Moredenite has an excellent characteristic due to its shape selectivity and low mesoporosity. Heterogeneous niobium catalysts (niobic acid, H_3PO_4 treated niobic acid and niobium phosphate) have recently been found to be selective catalysts for dehydration of polyols [12].

According to glycerol is a by-product of that biodiesel production but the demand for glycerol is not increasing at the same rate as the need for biodiesel. Consequently, the use of glycerol as a starting material becomes economically and environmentally feasible. The study on conversion of low value glycerol to higher value chemicals is interesting [13]. One attractive process is the conversion of glycerol to 1-propanol. In this process, glycerol is converted to 1-propanol via dehydration giving acrolein which then followed by hydrogenation yielding propionaldehyde and 1-propanol, respectively (Figure 2.5).

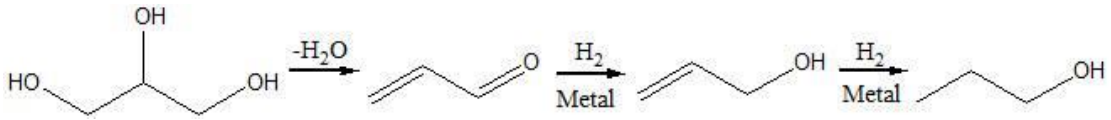

Figure 2.5 Pathway of glycerol to 1-propanol

Glycerol is mainly dehydrated at the secondary hydroxyl. As a result, an intermediate called 3-hydroxypropionaldehyde (3-HPA) would be formed and subsequently dehydrated to acrolein as major product. (Figure 2.6) This is because protonation of a secondary hydroxyl is more favorable over the Brönsted acid sites in the zeolite [15].

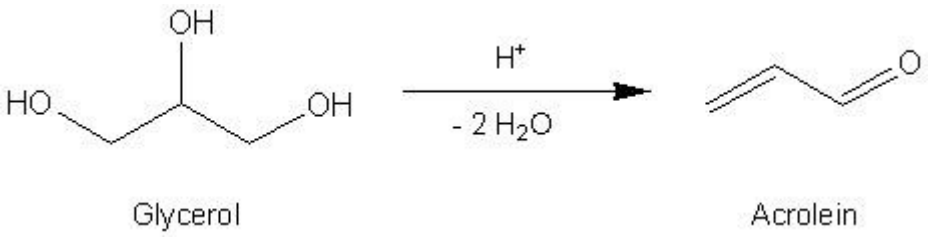

Figure 2.6 Acid-induced dehydration of glycerol to acrolein

The application of various types of catalysts in dehydration of glycerol to acrolein has been reporting recently including phosphates and pyrophosphates, mixed metal oxides, heteropoly acids, and zeolites.

Mixed oxides, phosphates and pyrophosphates catalysts are widely used in dehydration reaction of glycerol to acrolein. In fact, mixed oxides, phosphates and pyrophosphates catalysts has many parameters for evaluation and investigation during the optimization of catalytic activity [12]. Suprun *et al*., [14] demonstrated the different activity in the catalytic dehydration of glycerol in the gas-phase carried out at 280^{o}C with the presence of Al_2O_3 and TiO_2 supports modified by impregnation with PO^{-}_{4} ions and SAPO-11 and SAPO-34 samples as catalysts. The result showed that 72% acrolein selectivity was obtained from SAPO-34 catalyst and the lowest 37% acrolein selectivity was obtained from TiO_2–PO_4 catalyst. They also stated that the mesoporous Al_2O_3–PO_4 and TiO_2–PO_4 catalysts with large pore size exhibited high activity but limited selectivity towards acrolein. On the other hand, SAPO-11 and SAPO-34 catalysts with small micropores were less active but more selective. The small pores of SAPO catalysts favor an external surface reaction rather than a reaction inside the channels leads lowering activity and accelerating deactivation.

Al_2O_3–PO_4 and TiO_2–PO_4 catalysts possess much larger pores; therefore, the whole surface was available for the reaction for a much longer period of time.

One approach to obtain higher acrolein from glycerol is to use supported inorganic acids, such as heteropoly acids (HPAs) and phosphorous acid as catalysts. HPAs can be used as acid and oxidation catalysts in both solid and liquid states. HPAs are highly stable against humidity and air, low toxicity, highly soluble in polar solvents (water, acetones, and lower alcohols), and less corrosive [1].

Tsukuda *et al*. [3] studied the production acrolein from glycerol using HPA catalysts. This reaction takes place under atmospheric pressure at 275-325°C in the liquid-phase. The conversion is reached up to 100% with 74.1% acrolein selectivity. The high catalytic activity of this catalyst dues to the strong Brönsted acid sites of the HPA.

Moreover, the activity of liquid-phase dehydration of glycerol using zeolite was also studied by Oliveira *et al*. [15]. The reaction was carried out at 250°C, and 70 bar over different large pore molecular sieve including H-Y, H-β, mordenite, SBA-15, and ZSM-23. The activity had almost the same order of the acidity: H-Y > H-β > H-Mor > SBA-15 > ZSM-23. The lower the Si/Al ratio, the higher the activity: a large pore molecular sieves, H-Y showed high performance with 99.5% acrolein selectivity and 89.0% conversion; while, SBA-15 possessed weak acidity produced 84.0% acrolein selectivity with low conversion at 40.6%. They were reported that large pore zeolites possessing mild or strong acidic sites, as in the case of H-Y and H-β, were highly active for the production of acrolein. However, in the case of leached of the acidic sites led to deactivation. The small microporous mordernite and ZSM-23 had weak and strong acidic sites, but the one-dimensional structure of the channels contributed to the deactivation of the solids by coking. A mesoporous SBA-15 had a mild acidity was able to convert glycerol into acrolein with high selectivity. It also showed the significant deactivation through poisoning of the acidic sites and blocking by heavy glycerol derivatives.

In addition, Witsuthammakul also shows that the used of H-ZSM-5 zeolites in glycerol dehydration at 330–360°C, the conversion can be reached to 100% with an acrolein

selectivity of more than 70% [2]. Therefore, H-ZSM-5 zeolite is one of the promising catalysts in glycerol dehydration.

2.1.2 Zeolite

Composition and structure of zeolites [16, 17]

Zeolites are solid crystalline of aluminosilicates, which consist of SiO_4 and AlO_4^- tetrahedral, and interlinked to be three-dimension network of porous structure. They can be built by nature or synthesis. The inside of zeolites pore has metals or other cations, which balance negative charge from the anionic framework resulting from the containing aluminium. The general formula of zeolite is $M_v(AlO_2)_x(SiO_2)_y.zH_2O$; where, M stands for metal cations. The composition of zeolites is identified by the Si/Al atomic ratio or by molar ratio M ($M = SiO_2/Al_2O_3$)

The zeolites growth can be represented in Figure 2.7. The SiO_4 and AlO_4^- tetrahedral, which is defined as primary units, are polymerized to planar secondary units, then evolved to complex three-dimension unit called polyhedral e.g. cube, hexagonal and octahedral. These polyhedral are ultimately arranged in many connection modes to form porous structure (cages and channels) of zeolites, such as sodalite cage and supercage.

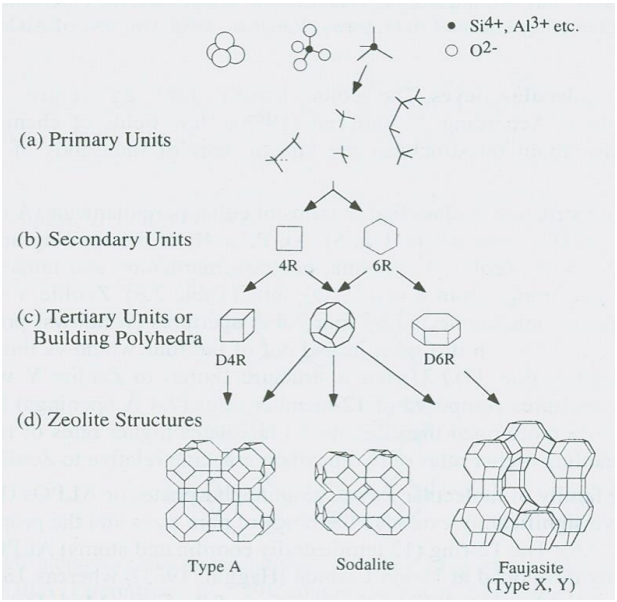

Figure 2.7 Formation of three common zeolites from primary units [16]

The pore of zeolites can be oriented in one, two or three dimensions (Figure 2.8) and aperture of pore depending on number of T-atom composition Si, Al, or other metals;

(see Table 2.1). The pore size can be changed by exchanging the cation in zeolites: for example, the aperture size of zeolites A can be modified to be 3, 3.8 and 4.3 Å when use K^+, Na^+, and Ca^{2+} as a balancing cation, respectively.

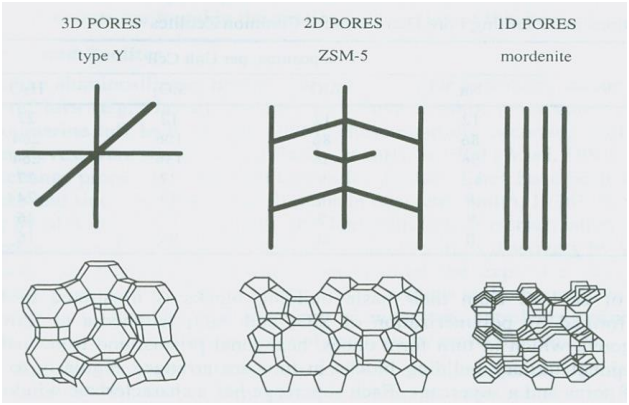

Figure 2.8 Three commercial zeolites of difference dimensionalities [16]

Table 2.1 Zeolites classified by window size [18]

Types	Small	Medium	Large	Extra large	Mesopore
Pore size (nm)	0.4 - 0.5	0.5 - 0.6	0.7 - 0.8	1.0 - 1.4	>2.0
T-atom	8	10	12	14-20	Variable
	Zeolite A	ZSM-5	Faujasite	CIT-5	MCM-41
	Chabasite	Theta-1	Cancrinite	VPI-5	MCM-48
	Rho	Ferrierite	Mordenite	Cloverite	
	Erionite	ZSM-11	Zeolite L		
	Zeolite P	ZSM-23	Offretite		
	Analcime		Beta		
	Philipsite		Gmelinite		

Zeolite synthesis

The first laboratory study the synthesis of a zeolite is attributed to Deville, who in 1862 synthesized levyne (levynite) $Ca_9[Al_{18}Si_{36}O_{108}]\cdot 50H_2O$ by heating potassium silicate and sodium aluminate in a glass ampoule. A large increase in synthesis of zeolites was seen after 1940 when X-ray diffraction became a common tool for analysis.

Zeolites are usually synthesized from a basic medium (sol or gel) under mild to medium hard hydrothermal conditions (70–350°C). They mainly obtained as powder as very small crystals. The important components for zeolite synthesis are: water, silica source, alumina source, pH-regulators, and templates (catalysts, nucleation centers).

Composition

- Temperature
- pH
- Temperature ramps
- Aging conditions
- Stirring rate
- Order of mixing

Zeolite synthesis is still mainly done by trial and error with some knowledge and experience.

2.1.3 H-ZSM-5 zeolite

ZSM-5 is an aluminosilicate zeolite belonging to the pentasil family of zeolites. Its chemical formula is $Na_nAl_nSi_{96-n}O_{192}\cdot 16H_2O$ ($0<n<27$), patented by Mobil Oil Company in 1975. It is widely used in the petroleum industry as a heterogeneous catalyst for hydrocarbon isomerization reactions [19].

ZSM-5 Structure

ZSM-5 is composed of several pentasil units linked together by oxygen bridges to form pentasil chains. A pentasil unit consists of eight five-membered rings. In these rings, the vertices are Al or Si, and an O is assumed to be bonded between the vertices. The pentasil chains are interconnected by oxygen bridges to form corrugated sheets with 10-ring holes. Like the pentasil units, each 10-ring hole has Al or Si as vertices with an O assumed to be bonded between each vertex. Each corrugated sheet is connected by

oxygen bridges to form a structure with “straight 10-ring channels running parallel to the corrugations and sinusoidal 10-ring channels perpendicular to the sheets”. Adjacent layers of the sheets are related by an inversion point. The estimated pore size of the channel running parallel with the corrugations is 5.4–5.6 Å. The crystallographic unit cell of ZSM-5 has 96 T sites (Si or Al), 192 O sites, and a number of compensating cations depending on the Si/Al ratio, which ranges from 12 to infinity. The structure is orthorhombic (space group P_{nma}) at high temperatures, but a phase transition to the monoclinic space group $P2_1/n.1.13$ occurs on cooling below a transition temperature, located between 27 and 77°C. The structure of ZSM-5 is shown in Figure 2.9.

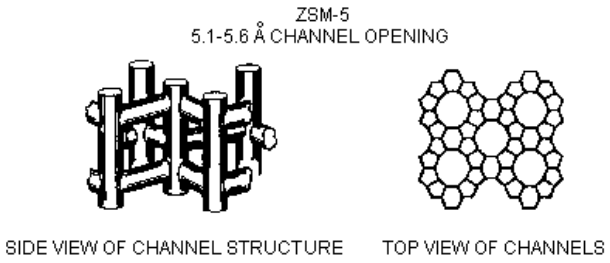

Figure 2.9 ZSM-5 structure

ZSM-5 Synthesis

ZSM-5 is a synthetic zeolite, closely related to ZSM-11. There are many ways to synthesize ZSM-5, a common reaction is as follows [20]:

$$SiO_2 + NaAlO_2 + NaOH + N(CH_2CH_2CH_3)_4Br + H_2O \longrightarrow \text{ZSM-5} + \text{analcime} + \text{alpha-quartz}$$

ZSM-5 is typically prepared at high temperature and high pressure in a Teflon-coated autoclave and can be prepared with various ratios of SiO_2 and Al containing compounds.

ZSM-5 catalyst was first synthesized by Argauer and Landolt in 1972. It is a medium pore zeolite with channels defined by ten-membered rings. The synthesis involves three different solutions. The first solution is the source of alumina, sodium ions, and hydroxide ions; in the presence of excess base the alumina will form soluble $Al(OH)_4^-$ ions. The second solution has the tetrapropylammonium cation that acts as a templating agent. The third solution is the source of silica, one of the basic building blocks for the framework structure of a zeolite. Mixing the three solutions produces supersaturated tetrapropylammonium ZSM-5, which can be heated to recrystallize and form a solid.

Uses of ZSM-5

ZSM-5 has high silicon to aluminum ratio. Whenever an Al^{3+}cation replaces a Si^{4+}cation, an additional positive charge is required to keep the material charge-neutral. With proton (H^{+}) as the cation, the material becomes more acidic. Thus, the acidity is proportional to the Al content. The very regular 3-D structure and the acidity of ZSM-5 can be utilized for acid-catalyzed reactions, such as hydrocarbon isomerization and alkylation. One such reaction is the isomerization of *m*-xylene to *p*-xylene. Within the pores of the ZSM-5 zeolite, *p*-xylene has a much higher diffusion coefficient than *m*-xylene. When the isomerization reaction is allowed to occur within the pores of ZSM-5, *p*-xylene is able to traverse along the pores of the zeolite, diffusing out of the catalyst more rapidly than the other one. This size-selectivity allows the isomerization reaction to occur quickly in high yield.

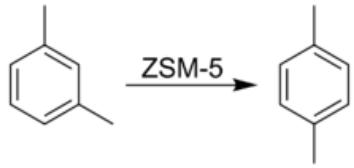

Figure 2.10 Selective isomerization of *m*-xylene to *p*-xylene using ZSM-5

ZSM-5 has been used as a support material for catalysis. In one such example, copper is deposited on the zeolite and a stream of ethanol is passed through at temperatures of 240 to 320°C as a vapor stream, which causes the ethanol to be oxidize to acetaldehyde; two hydrogens are releasing as hydrogen gas. It appears that the specific pore size of ZSM-5 is of benefit to this process, which also functions for other alcohols and oxidations. The copper is occasionally combined with other metals, such as chromium, to fine tune the diversity and specificity of the products. Acetic acid is an example of one possible byproduct from hot copper oxidation.

Zhou *et al.* [21] used micro and meso-porous ZSM-5 catalyst, which was synthesized by dual templates in one-step crystallization route, in glycerol dehydration to acrolein. They studied by compared the catalyst activity of ZSM-5, MCM-41, solid phosphoric acid, and the mixture of ZSM-5 and MCM-41 with the synthesized catalysts. The result showed that the highest 73.64% acrolein yield at 98.27% glycerol conversion was obtained from micro- and meso- porous ZSM-5. However, they concluded that meso-porous ZSM-5 was

more suitable than micro-porous since no diffusional limitation was observed for the meso-porous material.

In group previous work, Witsuthammakul and Sooknoi [2] successfully produced acrylic acid in a single reactor with subsequent oxidation of the glycerol dehydrated products. The selective dehydration of glycerol to acrolein was promoted by H–ZSM–5, H–β, H–mordenite, and H–Y catalysts at 275–400°C reaction temperature. The results indicated that H-ZSM-5 with medium pore size had a complete conversion of glycerol up to 81% acrolein.

According to the important of acrolein as an intermediate for chemical industry, which can be obtained from the dehydration of glycerol. In addition, acrolein has a storage problem, which handling requiring the highest safety standard. Therefore, to avoid such problematic ibstructiveness, acrolein, thus, should be converted to another more stable chemical feedstock immediately. The strategies are to convert acrolein to acrylic acid [2], propionaldehyde and unsaturated alcohol [22]. Peng *et al.* [23] studied the conversion of 1,2-propanediol to 1-propanol over a ZrNbO catalyst via dehydration and consecutive hydrogen transfer. They reported that ZrNbO species are active and selective catalysts for this reaction. The weak Brønsted acid sites for ligand exchange with the alcohol to form alkoxides on the catalyst. Propionaldehyde coordinates to the brønsted acid sites, activating the carbonyl group and initiating a hydride transfer from alcohol to the carbonyl. Then a ketone is formed and subsequent alcoholysis leads to the product, 1-propanol, and regeneration of the active catalyst.

The effects of the supports on hydrogenation and isomerization of allyl alcohol were investigated by Hoang-Van and Zegaoui [24]. In the hydrogenation of acrolein, allyl alcohol was significantly produced the reduced over Pt/MoO_3 and Pt/WO_3 catalysts in 400-573 K temperature of range. This supports created an adlineation sites as a result of an association of platinum atoms and electron-deficient. These adlineation sites, which contain electron-deficient cations resulting from a partial reduction of the oxide support, favor the isomerization of allyl alcohol to propionaldehyde with respect to its hydrogenation to propanol.

Volckmar *et al*. [25] investigated the gas phase hydrogenation of acrolein over supported silver catalysts with various SiO_2/Al_2O_3 ratios. They reported that at a high total

acidity and a high amount of strong Lewis acid sites on the catalysts showed a clear dependence on the support composition and can cause a low conversion of acrolein and low selectivity to allyl alcohol. This may result from the interaction of the metal with the Lewis acid sites of the support leading to a change in the hydrogenation properties of the silver by influencing hydrogen adsorption properties of acrolein.

2.1.4 Hydrogenation of aldehydes [26]

Aldehydes are usually easily hydrogenated to the corresponding alcohols over most of the transition metal catalysts. The rates of hydrogenation of carbonyl compounds depend on the nature of catalyst, the structure of compounds, and the reaction conditions.

Hydrogenation reaction [27]

Hydrogenation is a chemical reaction between molecular hydrogen (H_2) and another compound or element, usually in the presence of a catalyst, such as platinum, palladium or nickel. The process is commonly employed to reduce or saturate organic compounds. Hydrogenation typically constitutes the addition of pairs of hydrogen atoms to a molecule, generally an alkene. Catalysts are required for the reaction to be usable; non-catalytic hydrogenation takes place only at very high temperatures. Hydrogenation reduces double and triple bonds in hydrocarbons.

As a result of the importance of hydrogen, many related reactions have been developed for its use. Most hydrogenations use gaseous hydrogen (H_2), but some involve the alternative sources of hydrogen, not H_2: these processes are called transfer hydrogenations. The reverse reaction, removal of hydrogen from a molecule, is called dehydrogenation. A reaction where bonds are broken while hydrogen is added is called hydrogenolysis, a reaction that may occur to carbon-carbon and carbon-heteroatom (oxygen, nitrogen or halogen) bonds. Hydrogenation differs from protonation or hydride addition: in hydrogenation, the products have the same charges as the reactants.

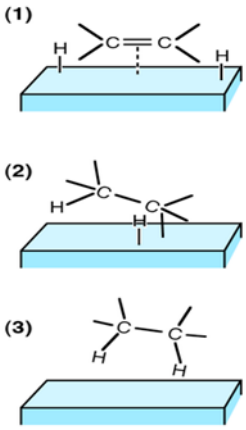

Figure 2.11 Steps in the hydrogenation of a C=C double bond at a catalyst surface, for example Ni or Pt.

Reaction conditions [26]

The successful performance of a catalytic hydrogenation depends on a suitable choice of reaction conditions, in particular, the choice of catalyst and its amount, temperature, hydrogen pressure, and solvent. Hydrogenation catalysts are also subject to deactivation or promotion by various substances that are referred to as inhibitory (or poisons) or promoters, respectively. In some case, the impurities of the substrate to be hydrogenated or the product may become a factor that retards the hydrogenation, usually in a later stage of the reaction.

Use of elevated temperatures and pressures is usually favorable for increasing the rates of hydrogenation and hence shortening the reaction time. Hydrogenations that proceed only slowly or not at all at a low temperature may be achieved successfully merely by raising the temperature (and also the pressure).

The effect of hydrogen pressure and rate of hydrogenation may depend on various factors, such as the catalyst, the substrate, the reaction conditions, etc. In most hydrogenations, however, increasing the hydrogen pressure is undoubtedly favorable for increasing the rate, reducing the reaction time, and an efficient use of catalyst.

2.1.5 Hydrogenation of acrolein to 1-propanol

The gas phase hydrogenation of acrolein is also an option for the industrial production of alcohols. The use of typical hydrogenation catalysts like Pt, Pd, or Ni supported on non-reducible oxides leads mainly to the saturated aldehyde as shown in the reaction in Figure 2.12, which is understandable since thermodynamics and kinetics favor the hydrogenation of the C=O and C=C bond.

Figure 2.12 Reaction pathway of acrolein hydrogenation

2.1.6 Hydrogenation catalysts [26]

Heterogeneous transition metal catalysts for hydrogenation are usually employed in the states of metal, oxides, or sulfides that are either unsupported or supported. The physical form of a catalyst suitable for a particular hydrogenation is determined primarily by the type of reactors, such as fixed-bed, fluidized-bed, or batch reactor. For industrial purpose, unsupported catalysts are seldom employed since supported catalysts have many advantages over unsupported catalysts. In general, use of a support allows the active component to have a larger exposed surface area, which is particularly important in those cases, where a high temperature is required to activate the active component. At that temperature, it tends to lose its high activity during the activation process, such as in the reduction of nickel oxides with hydrogen, or where the active component is very expensive as are the cases with platinum group metals. The effect of an additive or impurity appears to be more sensitive for unsupported than supported catalysts. This is also in line with the observations that supported catalysts are usually more resistant to poisons than unsupported catalysts. Supported catalysts may be prepared by a variety of methods, depending on the nature of active components as well as the characteristics of carriers. An active component may be incorporated with a carrier in various ways, such as, by decomposition, impregnation, precipitation, coprecipitation, adsorption, and ion exchange. Both low- and high-surface-area materials are employed as carriers. Some characteristics of commonly used supporting materials are summarized in Table 2.2

Table 2.2 Characteristics of commonly used carriers

Carrier	Specific Surface Area ($m^2 .g^{-1}$)	Pore Volumn ($ml . g^{-1}$)	Average Pore Diameter (nm)
α-Al_2O_3	0.1-5	-	500-2,000
Activated Al_2O_3	100-350	0.4	4-9
SiO_2-Al_2O_3	200-600	0.5-0.7	3-15
SiO_2	400-800	0.4-0.8	2-8
Zeolite	400-900	0.08-0.2	0.3-0.8
Activated carbon	800-1200	0.2-2.0	1-4

Nickel as a metal catalyst [26, 29]

Nickel is a very active metal in hydrogenation catalysis. It is also a cheap element, thus, allowing its use as a bulk metal (e.g. as Raney nickel) as well as in the form of highly loaded supported catalysts. This also rises to sulfur resistance, just because much sulfur is needed to fully poison highly loaded catalysts. On the other hand, the carcinogenic toxicity of nickel compounds is a big concern in the preparation and disposal of catalysts.

Many investigators have recognized that nickel oxide supported on kieselguhr gives much more activity catalysts than an unsupported one; although, the reduction temperature of supported oxide required in the range of 350–500°C.

Silica as a catalyst support [29,30]

In nature, silica can be found in a wide range of both crystalline and amorphous structures depending on the previous history of the sample. In all cases, the structure involves the connection of tetrahedral SiO_4 units so that different polymorphs showing the different relative orientation and coordination. This permits one to use cluster models to simulate SiO_2 surfaces since the different structures differ essentially in the long-range order which lead to the different crystalline and amorphous forms of silica. Additionally, the largely covalent character of this oxide facilitates a very simple representation by means of cluster models. In this case, part of the material is cut from the bulk of the most common

polymorph at ambient conditions, this being the alpha phase. This cut leads a series of dangling bonds either at silicon or at the oxygen atoms. Usually O atoms are preferred at the cluster edge since in this case the resulting dangling bond can be more realistically saturated by embedding hydrogen atoms. This is because the H electronegativity is relatively close to that of Si. The alternative option leads to unrealistic Si-H bonds, which strongly and artificially polarizes the rest of the material model. The orientation chosen for these embedded H atoms is in the line of the O-Si bond cut at atypical O-H bond. Furthermore, these terminal or capping atoms are kept fixed so as to reproduce the mechanical restrictions induced by the rest of the solid matrix. This strategy is commonly used to simulate other materials such as silicon or zeolites and has been reviewed at length by various authors.

According to the weak dispersing ability of silica, Ni on silica gives rise to Ni-metal particles weakly interacting with this quite inert “support”. Catalysts that contain up to 70% NiO with kieselguhr, amorphous silica or silica alumina in the fresh unreduced state. There are largely applied for a number of hydrogenations, such as oxoaldehydes to alcohols, reductive amination of carbonyls, alcohols and nitriles and nitro-compounds hydrogenation to amines.

Ni and copper catalysts supported on silica are largely used for hydrogenation. In most cases, indeed, the amount of silica is very small, being thus more a stabilizer than a support. As for example, 3% CuO, 68% NiO/SiO_2 is applied to oxoaldehydes hydrogenation processes to oxoalcohols (SC). 60% NiO/SiO_2 (NiSAT 320) are used as slurry application in the hydrogenation of nitro-compounds to anilines [31]. While similar catalysts from the same family (NISAT from Su¨d Chemie) are applied for benzene hydrogenation to cyclohexane, and nitriles hydrogenation to amines. Cu/SiO_2 and $CuCr/SiO_2$ are used for both hydrogenation of carbonyls and dehydrogenations of alcohols [32].

Activated carbon as a catalyst support [33, 34]

Activated carbon, also called activated charcoal, activated coal, or carbo activatus, is a form of carbon processed to have small, low-volume pores that increase the surface area available for adsorption or chemical reactions. Due to its high degree of microporosity, just one gram of activated carbon has a surface area in excess of 500 m^2, as determined by

gas adsorption. An activation level sufficient for useful application may be attained solely from high surface area; however, further chemical treatment often enhances adsorption properties. Activated carbon is usually derived from charcoal and increasingly, high-porosity biochar.

Impregnated carbon is a porous carbon containing several types of inorganic impregnate, such as iodine, silver. Moreover, cations, such as Al, Mn, Zn, Fe, Li, Ca have also been prepared for specific application in air pollution control. Due to its antimicrobial and antiseptic properties, silver loaded activated carbon is used as an adsorbent for purification of domestic water. Drinking water can be obtained from natural water by treating the natural water with a mixture of activated carbon and $Al(OH)_3$, a flocculating agent. Impregnated carbons are also used for the adsorption of hydrogen sulfide (H_2S) and thiols. Absorption rates for H_2S as high as 50% by weight.

Most carbonaceous materials have a certain degree of porosity and an internal surface area in the range of 10–15 m^2/g. During the activation, the internal surface becomes more highly developed and extended by controlled oxidation of carbon atoms - usually achieved by the use of steam at high temperature. After activation, the carbon will have acquired an internal surface area between 700 and 1,200 m^2/g, depend on the plant operating conditions. The internal surface area must be accessible to the passage of a fluid or vapor if a potential for adsorption is to exist. Thus, it is necessary that an activated carbon has not only a highly developed internal surface but also accessibility to that surface via a network of pores of differing diameters.

As a generalization, pore diameters are usually categorized as follows:

- Micropores < 40 Angstroms; 20 nm
- Mesopores 40–5,000 Angstroms; 2–50 nm
- Macropores > 5,000 (typically 5000- 20000 Angstroms); 50 nm

During the manufacturing process, macropores are first formed by the oxidation of weak points (edge groups) on the external surface area of the raw material. Mesopores are then formed and are, essentially, secondary channels formed in the walls of the macropore structure. Finally, the micropores are formed by attack of the planes within the structure of the raw material. All activated carbons contain micropores, mesopores, and macropores

within their structures but the relative proportions vary considerably according to the raw material.

Magnesiumoxide as a catalyst support [29]

Alkaline earth oxides (MgO, CaO, SrO, and BaO) are strong solid bases. Alkaline-earth oxides, except BeO, are among the strongest solid bases that may be stable as such in practical conditions. While BeO crystallizes into the wurtzite structure, with tetrahedral coordination for both $Be^{2+}$and O^{2-}, all other alkali-earth oxides crystallize in the rock salt-type "periclase" structure, with octahedral coordination of both cations and anions. The basicity of alkaline-earth oxides increases with the cation atomic number: in fact, increasing size and decreasing polarizing power of the cation results in an increased rock-salt-type unit cell size as well as in decreasing Madelung potential, thus destabilizing the oxide anions. This is reflected, e.g., on the increased temperature for carbon dioxide desorption, taken as a measure of surface basicity.

MgO powders can also be prepared by oxidation of Mg metal in different ways. These different preparation procedures give rise to very different particle morphologies [35,36]. In particular, MgO smoke produced by burning Mg has low surface-area nonporous particles with cubic habit and (100) terminations. Due to theirs smaller but still cubic particles can be obtained by decomposing $Mg(OH)_2$ produced by MgO rehydration as well as by Chemical Vapor Deposition, CVD, of MgO from Mg vapor. When produced by thermal decomposition of the hydroxycarbonate, the crystal habit is different but apparently still (100) terminations predominate. Instead, MgO arising from precipitated $Mg(OH)_2$ (brucite) tends to retain the lamellar structure of the hydroxide and may expose (111) terminations.

The size of Mg^{2+} is sufficiently small to enter close packing of oxygen ions, ccp and hcp. For this reason, Mg ions can participate to the formation e.g., of mixed oxides, such as spinels and ilmenites. whose oxygen packings are ccp and hcp, respectively. In relation with this, the deposition of Mg ions at the surface of normal carriers such as alumina. For example, alumina may give rise to poor stability due to the easy reaction producing Mg aluminate, arising from the penetration of Mg ions into the ccp oxygen packing of alumina.

Due to their strong basicity, alkali-earth oxides cannot be covered by "monolayers" of other more covalent oxides. In contrast, with what happens with ionic but less basic

oxides, such as zirconia, titania, alumina, where oxide-supported-on oxides can be prepared. In practice, the deposition of vanadate, tungstate, molybdate, sulfate, silicate and borate species on MgO and other alkali-earth oxides gives rise easily to bulk salts more than supported oxides. Reactivity is strong also with ionic oxides, such as, NiO, FeO, CoO, CuO, that tend to produce solid solutions with MgO and higher alkali-earth oxides.

Layered Double Hydroxide as a catalyst support [37]

The basic layer structure of layered double hydroxides (LDHs) is based on that of brucite [$Mg(OH)_2$], typically associated with small polarizing cations and polarizable anions. It consists of magnesium ions surrounded approximately octahedrally by hydroxide ions. These octahedral units form infinite layers by edge sharing, with the hydroxide ions sitting perpendicular to the plane of the layers as shown in Figure 2.13. The layers then stack on top of one another to form the three-dimensional structure. From the point of view of close-packing, the structure can be said to be composed of close-packed plane of hydroxyl anions that lie on a triangular lattice. The metal cations occupy the octahedral holes between alternate pairs of OH planes and thus occupy a triangular lattice identical to that occupied by the OH ions. In actual fact, both the local geometry around the metal and the close-packing of the hydroxyl anions are strongly distorted away from the idealized arrangements. The octahedral are compressed along the stacking axis. This has the effect of increasing the O-O and Mg-Mg distances parallel to the plane and to 0.3142 nm (experimental distance) and decreasing the thickness of the layers from 0.2427 to 0.2112 nm, with the O-M-O bond angles becoming 96.7°C and 83.3°C.

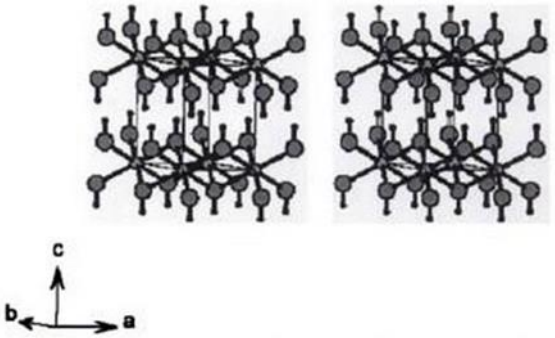

Figure 2.13 Stereographic projection of brucite [38]

Titanium dioxide as a catalysts support [29,30]

Titanium dioxide TiO_2 is a semiconductor oxide, for which four different polymorphs exist at normal conditions: rutile or anatase. Even if anatase has better chemical properties, including those related to photochemistry, rutile is easier to model from a computational point of view. Rutile is also the ground state under ambient conditions although for small crystallites the lower surface energy of the anatase faces with respect to those of rutile can led to formation of anatase quite frequently using some preparations. Rutile has a layered structure and the (110) surface is non-polar in nature and was one of the first oxides where STM measurements were successfully carried out and the images simulated through the use of theoretical methods and the Tersoff-Hamann formalism.

Medium-to-high surface area anatase is largely used as support of catalysts. The instability of anatase toward phase transformation into rutile does not allow its use for high-temperature reactions. In case of reaction temperatures 300─400°C normal high-area anatase may be used, in particular when anatasestabilizing components (such as silicate, molybdate, wolframate species or alkali or rare-earth ions) are also present. Mesoporous very high surface-area anatase may offer good opportunity for relatively low-temperature reactions such as, e.g., low-temperature CO oxidation over titania-supported noble metals.

γ-Alumina as a catalyst support [29]

Among the different transition alumina known, γ-alumina (γ-Al_2O_3) is perhaps the most important with direct application as a catalyst and catalyst support in the automotive and petroleum industries. The usefulness of this oxide can be traced to a favorable combination of its textural properties, such as surface area, pore volume, and pore size distribution and its acid/base characteristics. In addition, it is mainly related to surface chemical composition, local micro structure, and phase composition. Nevertheless, the chemical and hydrothermal stability of γ-Al_2O_3 are still a critical point for catalytic applications.

The surface interactions for small ions are generally accepted to be predominantly electrostatic, which is supported by experimental results where the extent of adsorption of positive/negative ions increases with a pH rise/decrease. Nevertheless, some experimental

evidence reflects exceptions from the simple rule of electrostatic adsorption with the existence of “specific” or “chemical” surface–adsorbate interactions. It may compete with coulombic repulsion, as in the adsorption of cations, such as Ni^{2+}, Co^{2+}, and Pb^{2+} onto a positively charged alumina surface. These results support the existence of specific sites on the hydroxylated surface that act in adsorption of the catalyst precursor and are related to the intrinsic acid/base properties of the surface.

γ-Al_2O_3/H_2O Interface

The existence of Lewis acid sites (cus cations) and basic sites (oxide anions) at the γ-Al_2O_3 surface allows its rehydroxylation (or rehydration) by interaction with H_2O, so that cus cations and anions can, in part, be converted into surface hydroxy groups. This interaction has been represented as a two-step process for γ-Al_2O_3 under atmospheric conditions that involves non-dissociative adsorption of H_2O on Lewis sites, which essentially consists in a transfer of electron density to a Lewis acid site.

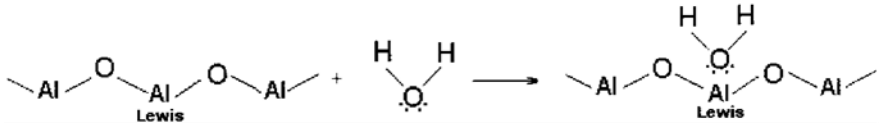

Figure 2.14 Dissociative chemisorption of H_2O and modification of Al surface

Followed by dissociative chemisorption of H_2O and modification of surface Al coordination with the hydroxy group bonded to the Al atom, i.e., the two-coordinate oxygen atom adjacent to the Al site is protonated.

Figure 2.15 The dehydration of γ-alumina

The rehydration of γ-alumina corresponds to the loss of tetrahedrally coordinated Al surface species and an increase of hydroxylated octahedral that can also involve some Al. The reactivity towards water depends on the layers exposed at each surface [39].

However, nickel and other metals are not really dispersed on alumina Ni tends to be dispersed atomically to some extent, producing hardly reducible surface cations that can give rise even to isolated metal centers or small clusters. At intermediate loadings, NiO is observed by XRD on the unreduced catalyst, but other techniques (such as TPR and UV)

reveal a behavior different than that of "normal" NiO particles; small metal particles predominate on the corresponding reduced catalysts. When loading is high, particles similar to unsupported NiO are also present in the unreduced catalyst, quite large Ni crystals being formed upon reduction. Interestingly, in some cases, hexagonal nickel is produced instead of cubic nickel, possibly because of a stabilization of hexagonal phase by carbon species.

A porous structure of the support also increases the stability of the metal. On comparing α-Al_2O_3 with γ-Al_2O_3, and SiO_2 and MgO of different porosities, Lu *et al*. [40,41] concluded that porous support favors metal dispersion and contact between the active sites and reactants, increasing the activity for CO_2 reforming and stability. This is also clear when a commercial y-Al_2O_3 support was compared with a γ-Al_2O_3 prepared by the sol-gel method [42]. Nickel supported on both aluminas had similar activity, but the stability of the catalyst prepared by sol-gel was higher. It can be explained in terms of the low particle size of the metal, which is below a critical value (10nm) that is the lowest limit for the formation of carbon on the nickel surface.

The effect of the support has been also investigated for other active metals, and the tendencies are not the same in all cases. Bitter *et al.* [43] found that the trend in stability on supported platinum was ZrO_2 > TiO_2 > Al_2O_3. This trend was different in supported nickel, with Al_2O_3 supported nickel being more stable than the corresponding TiO_2 supported catalyst [44]. In the case of Pt, there is no evidence of sintering, and deactivation is produced by blocking of the active centers by carbon. The support in this case have a very active role, and for the reducible oxides (TiO_2, ZrO_2), small oxide crystallites decorate the metal particle, producing a better control of carbon formation at this interface. Zhang et al. [45] found that the activity for CO_2 reforming in supported Rh catalyst followed the order: YSZ > Al_2O_3 > TiO_2 > SiO_2 > La_2O_3 > MgO, which is directly correlated with the acidity of the support. Deactivation is controlled by other parameters since in a specific support, it decreases when the particle size of Rh increases. Nevertheless, the nature of the support has a stronger influence on the catalytic life-time, which is low for TiO_2 and MgO within the mentioned support series. The latter data contrast with the results for nickel catalysts, where MgO is an excellent catalyst owing to the formation of the Ni-Mg-O solid solution. The formation of this solid solution is not favored in the Rh-Mg system. Also, some differences are found for supported Ir catalysts, with an activity trend is in the order TiO_2 >ZrO_2 >Y_2O_3 > MgO > Al_2O_3 > SiO_2.[46] Bradford and Vannice [47] studied

CO_2 reforming over different active metals (Ni, Co, Fe, Rh, Pd, Ir, Pt) supported on TiO_2 and SiO_2. The activity depended on the d-character of the transition metal, but the activity maximum was different for each support: Rh for TiO_2 and Pt in the case of SiO_2.

Chen *et al*. [48] was studied supported nickel catalysts with different supports, such as MgO, SiO_2, Al_2O_3, MgAlO and SiAlO for hydrogenation lauronitrile. They found that nickel was easier to reduce in Ni/MgO and Ni/SiO_2 than in Ni/Al_2O_3. They reported that acetonitrile was found to be adsorbed on the reduced nickel and acidic sites. The strong surface basicity of Ni/MgO was found to favor the selectivity to the primary amine, but inhibited the conversion of lauronitrile. On the other hand, the conversion of lauronitrile was high over the Ni/SiO_2 (93%), Ni/Al_2O_3 (97%) and Ni/SiAlO (94%) with strong surface acidity, but the selectivity to the primary amine was relatively low. The Ni/MgAlO with intermediate strengths of surface acidity and basicity exhibited the high conversion of lauronitrile and high selectivity to the primary amine.

2.1.7 Propanol [49]

1-Propanol, is a primary alcohol with the formula $CH_3CH_2CH_2OH$ (Figure 2.14). This colorless liquid is also known as propan-1-ol, 1-propyl alcohol, *n*-propyl alcohol, and *n*-propanol. It is an isomer of isopropanol (2-propanol, isopropyl alcohol). It is formed naturally in small amounts during many fermentation processes and used as a solvent in the pharmaceutical industry mainly for resins and cellulose esters.

Figure 2.16 Structure of propanol

Table 2.3 Physicochemical properties of propanol at 20°C

Chemical formula	C_3H_8O
Molecular mass	60.10 g/mol
Density	0.803 g/mL
Viscosity	1.938 mPa.s
Melting point	-126 °C
Boiling point	97 to 98 °C
Vapor pressure	1.99 kPa

Figure 2.17 shows the normal reactions of a primary alcohol. Thus, it can be converted to alkyl halides, for example red phosphorus and iodine produce *n*-propyl iodide in 80% yield; while PCl_3 with catalytic $ZnCl_2$ yields 1-chloropropane. Reaction with acetic acid in the presence of H_2SO_4 catalyst under Fischer esterification conditions gives propyl acetate however refluxing propanol overnight with formic acid alone can produce propyl formation in 65% yield. Oxidation of 1-propanol using $Na_2Cr_2O_7$ and H_2SO_4 produces only 36% yield of propionaldehyde. Oxidation with chromic acid yields propionic acid.

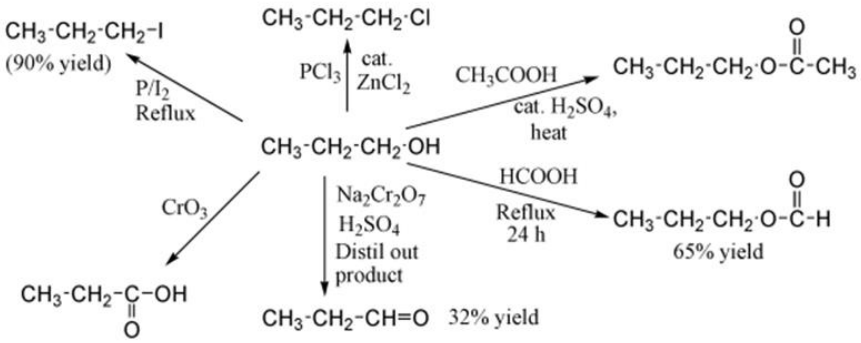

Figure 2.17 Normal reaction of n-propanol

2.2 งานวิจัยที่เกี่ยวข้อง

1-propanol is expected as a major product in our presence work. Acrolein from the upper catalytic bed is converted to 1-propanol via hydrogenation over metal catalysts; such as Ni, Cu and Pt under hydrogen pressure. Accordingly, continuous fixed-bed reactor is used to operate two-step process. Upper bed is dehydration reaction by acid catalysts and lower bed is for the hydrogenation of acrolein using supported Ni catalyst.

Ryneveld *et al*. [50] investigated the production of lower alcohols from glycerol using Ni supported on silica and alumina as catalysts with temperature and pressures between 230–320°C and 40–75 bar, respectively. They found that Ni/SiO_2 gave quantitative conversion of glycerol at a lower temperature compared to Ni/Al_2O_3. Ni/SiO_2 also gave a higher selectivity to ethanol and propanol (63%) compared to Ni/Al_2O_3 (52%) at a similar conversion. The used catalyst showed sintering of the Ni, which was confirmed by a loss of surface area and average crystallite size due to high %loading of Ni content. The route to lower alcohols from glycerol is proposed to occur via 1,2-propanediol.

Since acrolein can be converted to 1-propanol via hydrogenation over metal catalysts; such as Ni, Cu and Pt under hydrogen pressure. Accordingly, 1-propanol production from glycerol in the continuous fixed-bed reactor was used to operate. The upper bed was the dehydration reaction by acid catalysts and lower bed was hydrogenation by metal catalysts over various supports such as silica, alumina, titania, LDH, magnesium oxide, and activated carbon.

บทที่ 3

วิธีดำเนินการวิจัย

3.1 Chemical reagents

Chemical reagents	Grade of purity	Manufacturers
1. Nickel(II) nitrate hexahydrate	99%	CARLO ERBA
2. Nickel (II) chloride	≥98.0%	Fluka
3. NH_4-ZSM-5 (Si/Al = 12.5)		Zeochem
4. Silica	99.0% on dry	CARLO ERBA
5. Aluminium hydroxide	90%	Panreac
6. Titanium dioxide		TOA Paint
7. Magnesium oxide	>98.0%	Fluka
8. Layered double hydroxides		SCG Chemical
9. Activated carbon		Merck
10. Glycerol	99.5%	CARLO ERBA
11. N-butanol	99.5%	CARLO ERBA
12. Distillation water		

3.2 Apparatus and instruments

1. Catalytic testing rig
2. Gas chromatograph (VARIAN CP-3800)
3. Laboratory glassware
4. Laboratory plasticware
5. Oven
6. Sieve
7. Syringe (10 mL)
8. Syringe pump
9. Mass flow controller
10. Cooling water
11. Tube furnace with a programmable temperature controller
12. Temperature programmed reduction (TPR) system
13. Temperature programmed desorption (TPD) system
14. X-ray fluorescence spectrometer (XRF)
15. X-ray Diffractometer (XRD)
16. Transmission electron microscopy (TEM)
17. Thermal gravimetric analysis (TGA)

3.3 Catalyst Preparation and modification

3.3.1 Preparation of H-ZSM-5 Support

A powder of NH_4-ZSM-5 was calcined in the tube furnace with programmable temperature controller at 500°C for 5 h to make a proton form; H-ZSM-5 with Si/Al ratio of 12.5. H-ZSM-5 was used as a catalyst for the first catalytic bed of dehydration reaction.

3.3.2 Preparation of 20 wt.% Ni supported silica (SiO_2), γ-alumina (γ-Al_2O_3), titanium dioxide (TiO_2), magnesium dioxide (MgO) and layered double hydroxides (LDH) catalysts.

Before impregnation, all of the supports were dried at 80°C in an oven for 24 hour in order to remove moisture and impurity. Aluminiumhydroxide was calcined in a tube furnace at 550°C for 5 h to make γ-Al_2O_3.

The 2 M Ni precursor solution was prepared by dissolving 9.9000 g of $Ni(NO_3)_2$•$6H_2O$ in 17 mL of water. After that, 8.0000 g of SiO_2, γ-Al_2O_3, TiO_2, MgO, and LDH was impregnated with the Ni precursor solution in plastic beaker. The mixture was gradually dried in an oven at 100°C to remove excess water till support almost dry. Then, it was calcined in a tube furnace at 500°C for 5 h to obtain NiO, reduced at 450°C for 3 hour to Ni metal form.

3.3.3 Preparation of 20 wt.% Ni supported activated carbon catalyst (Ni/C)

Ni supported on activated carbon catalyst was also prepared by using the same procedure that described above. Nickel (II) chloride ($NiCl_2$) was used as a Ni precursor. 9.9000 g Nickel (II) chloride was dissolved in 17 mL water to make metal solution. After impregnation the catalyst was dried at 100°C overnight, followed by calcination at 500°C for 5 hour under nitrogen pressure in a fixed-bed reactor. Then, H_2 was used to reduce the catalyst at 450°C for 3 hour.

3.4 Characterization of catalysts

3.4.1 X-ray diffraction (XRD)

X-ray diffraction (XRD) is the technique used for determined crystal structure of the catalysts. CuK_α was used as analytical X-ray source at 30 kV and 40 mA. The sample is prepared by spreading catalyst over sample holder and placed into the instrument. The

XRD analysis was scanned from 2θ = 5 to 90°C with 1 sec/step time and 0.04 2θ/step increment.

3.4.2 X-ray fluorescence (XRF)

X-ray fluorescence (XRF) is the emission of characteristic "secondary x-ray" (or fluorescent), which is x-rays from a material that has been excited by bombarding with high-energy X-rays. Each element has electronic orbitals of characteristic energy. The removal of an inner electron by an energetic photon was provided by a primary radiation source, following by the moving of an electron from an outer shell into that vacancy and released energy call secondary electron or fluorescent. The released energy is a characteristic radiation that tells the composition of the sample. This technique can be done according to the following procedure: 0.5 g of catalyst sample was mixed with 4.5 g boric acid, and compressed into alumina pan before bring into the XRF sample holder in XRF instrument.

3.4.3 N_2-Gas adsorption analysis

Gas adsorption analysis is the technique generally used for determining surface area and pore size distribution of a solid catalyst. This technique can be done according to the following procedure: the catalyst sample was weighed about 100 mg and transferred to a cleaned, dried sample cell. This sample cell was attached to the outgassing station. Then, a heating mantle was installed with the sample cell and the temperature was raised to 300°C for 12 h. After the residual gas was removed by heating under vacuum, nitrogen adsorbate was filled by opening the gas inlet valve. The sample cell was attached to the sample station. Initially, a dewar flask of liquid nitrogen was placed around the sample cell. Nitrogen adsorbate pressure can be regulated by 1 torr transducer with 3 minutes equilibration time and 0 scaled tolerances. .

3.4.4 Temperature programmed reduction (TPR)

Temperature-programmed reduction (TPR) provides information on the active site species of the catalysts by monitoring their reducibility. Temperature programmed reduction was measured using thermal conductivity detector (TCD). The sample weighed 0.1 g was placed into a quartz tube reactor, which was located inside a temperature-regulated furnace. Prior to the H_2 - TPR, each sample was heated to its calcinations temperature in air zero for 3 h (25 mL/min) and cooled to 50°C. The heating rate of 2°C/min, the 5% H_2 in Ar flow of 25 mL/min was applied for TPR analysis. Water produced during the reduction process will be removed in a U-shape glass trap at -70°C (vapor of liquid N_2) before entering the TCD.

3.4.5 Temperature programmed desorption (TPD)

Ammonia is probably the most frequently used probe molecule for acidity assessment. Its small molecular size allows one to probe almost all acid sites of both micro and mesoporous materials. NH_3 - temperature-programmed desorption (NH_3 - TPD) experiments was carried out using a TCD detector. Before adsorption, the sample (0.2 g) as heated to its calcinations temperature in air zero for 2 h (30 mL/min) and cooled to 30°C. The adsorption of NH_3 was performed at 30°C. After saturation, the sample will be flushed with He at this temperature for 1 h. TPD measurements was done from 35 to 800°C with a heating rate of 10°C/min, using He as a carrier gas.

3.4.6 Transmission electron microscopy (TEM)

Transmission electron microscope (TEM) was used to study the morphology of catalyst and dispersion of metal supported catalyst. TEM uses a beam of highly energetic electron (voltage 80–120 kV) and signals from TEM depending on the sample density and thickness. Electrons that pass through the sample without energy loss it shows bright filed image and electrons are diffracted (scattered) by particles obtain dark-field images at magnification of 100,000–120,000x.

3.4.7 Thermal gravimetric analysis (TGA)

A Perkin-Elmer thermogravimetric analyzer recorded the mass loss of the sample after being heated to a high temperature. Approximately 10-15 mg of the powder was loaded to the platinum pan, after which the instrument read the exact mass. The sample was then heated from room temperature to 900ºC at the heating rate of 10ºC/min under the flow of nitrogen gas (40 mL/min). The mass of the powder was recorded as a function of time and temperature.

3.5 Catalytic Activity testing

3.5.1. Dehydration of glycerol to acrolein

The H-ZSM-5 Zeolite pellets was packed into the glass reactor (8 mm of inside diameter) and covered by glass wool. The glass beads were loaded under the H-ZSM-5 zeolite bed to facilitate feed flow dispersion.

The catalytic testing rig is shown in Figure 3.1. The reactor was positioned at the center of a vertical tube furnace. The gas flows will be controlled by mass flow controllers and checked by bubble flow meter. The catalyst was activated by heating at 2°C/min to 500°C and held at that temperature for 5 h under the steam of air zero (60 mL/min). After that, the reactor was cooled down to the reaction temperature (300°C). To start the reaction, glycerol solution (10 wt.%) was fed into the reactor by syringe pump at 1.7 mmol/h. The reaction was operated for 6 h on steam and collected hourly.

3.5.2 Subsequent hydrogenation of glycerol dehydrated products

The zeolite H-ZSM-5 and the supported Ni catalysts were sequentially packed in double-bed reactor. Each bed was screened by glass wool. The glass rod was inserted under the lower bed. The glass beads were introduced as flow dispersing between the zeolite H-ZSM-5 and supported Ni catalyst bed.

The double bed tubular down flow reactor was placed within a vertical tube furnace as explained previously. Hydrogen flow rate was controlled by a mass flow controller. The catalyst was reduced at 10°C/min to 450°C and held at that temperature for 3 h under hydrogen flow rate of 100 mL/min. Then, the reactor was cooled to the reaction temperature prior for testing. After that, the catalyst was purged by hydrogen for half an h under 100 mL/min. Glycerol solution (10 wt.%) was fed into the reactor by syringe pump with the flow rate 1.7 mmol/h. The reaction was operated for 6 h on steam. The product effluents will be condensed in the condenser by the coolant and collected hourly.

The description of the reaction set up and the reaction condition are summarized in Table 3.1

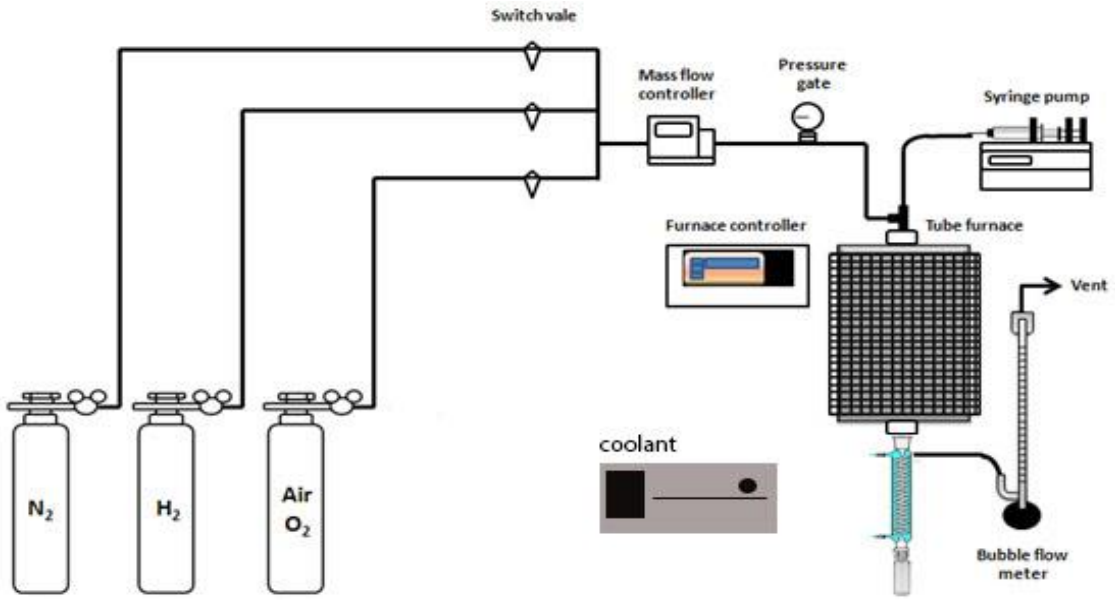

Figure 3.1 The schematic diagram of the catalytic testing rig

Table 3.1 Description of the reactor set up and the reaction conditions

Parameters	Value
Reactor inside diameter (mm)	6
Reactor outside diameter (mm)	8
Total flow (mL/min)	100
Bed length (cm)	25
Catalyst weight (g)	0.3
Contact time: W/F (g.h/mol)	15, 29, 59, and 177
Catalyst activation (before reaction)	Heating rate: 2°C/min
	Heat treatment: 500°C hold for 5 hours
	Gas: air zero (60 mL/min)
Carrier gas	H_2
Reaction temperature	100-200°C
Total reaction pressure	Atmospheric pressure

3.6 Products analysis

Products were quantified by gas chromatograph equipped with flame ionized detector (GC-FID Varaince CP-3800). DB-WAX (length, 30 m; internal diameter, 0.25 mm; film thickness, 0.25 um) was used as a separating column. The following temperature program; linear velocity is 21.9 cm/sec, 60°C hold for 2 min, then ramp at 8°C/min to 200°C was used for the analysis of liquid hydrocarbon and held at this temperature for 0.5 min by use N_2 as carrier gas. The products were mixed with equal weight of n-butanol as an internal standard. The mixture was injected at 0.1 μL and 200 of split ratio.

บทที่ 4

ผลการวิจัย

4.1 Catalyst characterization

The elemental composition of the catalysts is determined by X-ray fluorescence spectroscopy and the surface area is determined by N_2-physisorption as shown in Table 4.1.

Table 4.1 Ni content and surface area of catalysts and support

Catalyst	Ni (wt.%)	Surface area (m^2/g)	
		blank	Ni loaded
Ni/SiO_2	21.1	363	225
Ni/Al_2O_3	22.0	278	152
Ni/TiO_2	20.9	77	60
Ni/LDH	22.8	170	134
Ni/MgO	23.3	143	50
Ni/C	-	1,350	1,069

From Table 4.1, it can be seen that Ni loading in the catalysts is slightly higher than the expected value; that is 20 wt.%. It is suggested that for all of the catalysts, nickel loading is comparatively in the same range.

The BET surface area of SiO_2, Al_2O_3, TiO_2, LDH, MgO and activated carbon is found to be 250, 278, 77, 170, 143 and 1350 m^2/g, respectively. This means that SiO_2, Al_2O_3, and

activated carbon would be high surface area support. However, the surface area of 20 wt.% Ni/SiO_2, Ni/Al_2O_3, Ni/TiO_2, Ni/LDH, Ni/MgO and Ni/C are decreased upon metal loading. This is because nickel surface area is low, hence total surface area is decreased when low surface component is loaded.

4.1.1 Temperature Program Reduction Characteristics

Temperature programmed reduction profiles of 20 wt.% Ni/SiO_2, 20 wt.% Ni/Al_2O_3, 20 wt.% Ni/TiO_2, 20 wt.% Ni/LDH, 20 wt.% Ni/MgO and 20 wt.% Ni/C catalysts were investigated by H_2-temperature programmed reduction (H_2-TPR). The H_2-TPR profile of those catalysts prepared by impregnation method is shown in Figure 4.1.

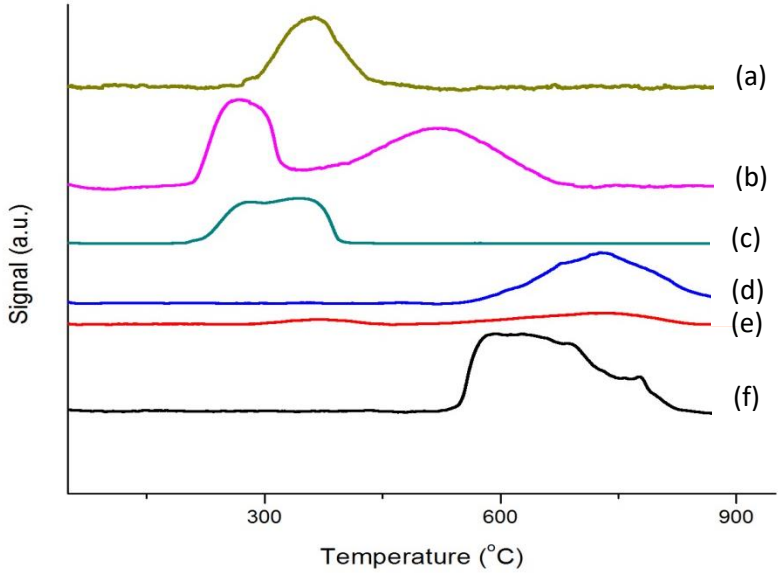

Figure 4.1 TPR profiles of (a) Ni/SiO_2, (b) Ni/Al_2O_3, (c) Ni/TiO_2, (d) Ni/LDH, (e) Ni/MgO, and (f) Ni/C

As seen from Figure 4.1, Ni/SiO_2 shows the reduction of Ni^{2+} to metallic Ni as shown in reduction peak at 380°C. For Ni/Al_2O_3 catalyst, it exhibits two reduction peaks at 250 and 500°C, the peak at 250°C can be referred to metallic Ni. The broad peak in the temperature range of 300-650°C exhibits the reduction of Al_2NiO_4 species [50]. It is suggested that Ni have a good interaction with Al_2O_3. For Ni/TiO_2 catalyst, it shows reduction peaks at the temperature of 200-400°C. This peak is assigned to the reduction of NiO to metallic Ni. For Ni/LDH catalyst, it shows reduction peak at 600-900°C, which show the reduction of Al_2NiO_4

and $MgNiO_2$ species. This could be referred Ni having a good interaction with LDH structure. For Ni/MgO catalyst, it exhibited two reduction peaks at 300 and 650°C, the peak at 300°C can be referred to metallic Ni. The broad peak in the temperature range of 600-900°C exhibits the reduction of $MgNiO_2$ species. For Ni/C catalyst, it shows reduction peak at the temperature of 550-750°C. This peak is assigned to the reduction of Ni-Carbide.

4.1.2 Temperature Program Desorption Characteristics

Ni/Al_2O_3 and Ni/TiO_2 were tested for the acidity using NH_3-TPD as shown in Figure 4.2.

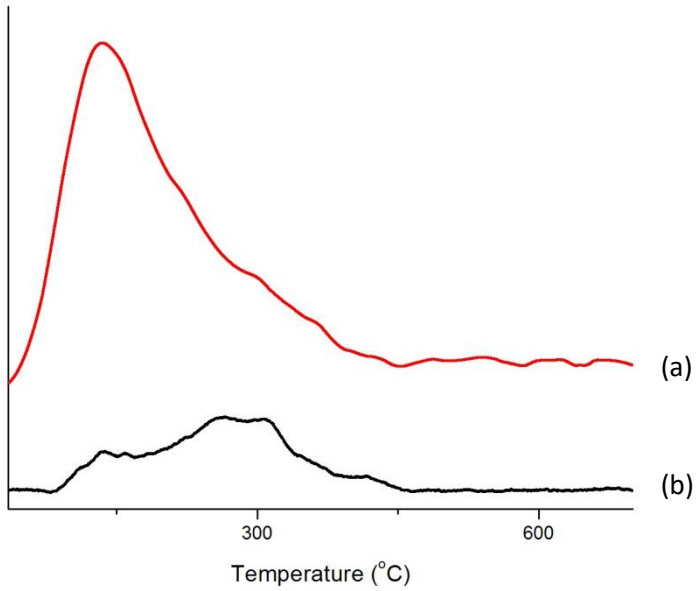

Figure 4.2 NH_3-TPD profiles of (a) Ni/Al_2O_3 and (b) Ni/TiO_2

From Figure 4.2 the thermal desorption of physisorbed ammonia on the surfaces take place at about 100°C for both catalysts. The broaden peak at low temperature (150-200°C) is attributed to the desorption of weakly bound ammonia; while, NH_3 desorption from strong acid sites takes place at 200-450°C. For weak acidity, the intensity of the acid sites of Ni/Al_2O_3 catalyst is higher than Ni/TiO_2 catalyst. This is because Ni/Al_2O_3 consists of high defect surface, as compared to Ni/TiO_2. For strong acidity, intensity of the acid sites of Ni/Al_2O_3 catalyst was similar to Ni/TiO_2 catalyst. However, the overall acidity of Ni/Al_2O_3 catalyst was greater than that of Ni/TiO_2 catalyst.

Ni/LDH and Ni/MgO were tested for the basicity using CO_2-TPD as shown in Figure 4.6. There was no acidity and basicity test for the neutral Ni/SiO_2 and Ni/C.

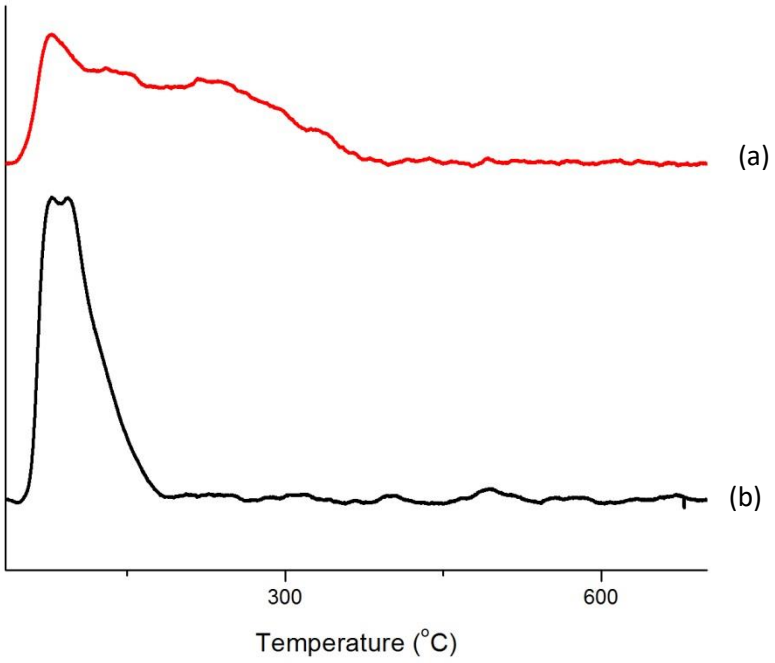

Figure 4.3 CO_2-TPD profiles of (a) Ni/LDH and (b) Ni/MgO

From Figure 4.3, the result shows the desorption of physisorbed CO_2 on the surfaces taking place at 75°C for both catalysts. The low temperature broaden peak (75-150°C) is attributed to the desorption of weakly bound CO_2 on the basic site. Ni/LDH takes place at 200-450°C because it occurs from Al or Mg carbonate species; while, no carbonate is found in Ni/MgO. The intensity of the basic sites of Ni/MgO catalyst was higher than that of Ni/LDH catalyst.

4.1.3 X-ray diffraction (XRD)

The catalysts prepared by wetness impregnation method after calcined at 450 °C were determined by X-ray power diffraction technique (XRD). In order to identify the crystal structure, 2θ angle in XRD diffraction pattern of each catalyst were compared with those of the reference diffraction pattern. The catalysts were scanned over the angle range (2θ) from 5° to 90°. The X-ray powder diffraction patterns of the metal oxide supported on silica catalysts are shown in Figure 4.4.

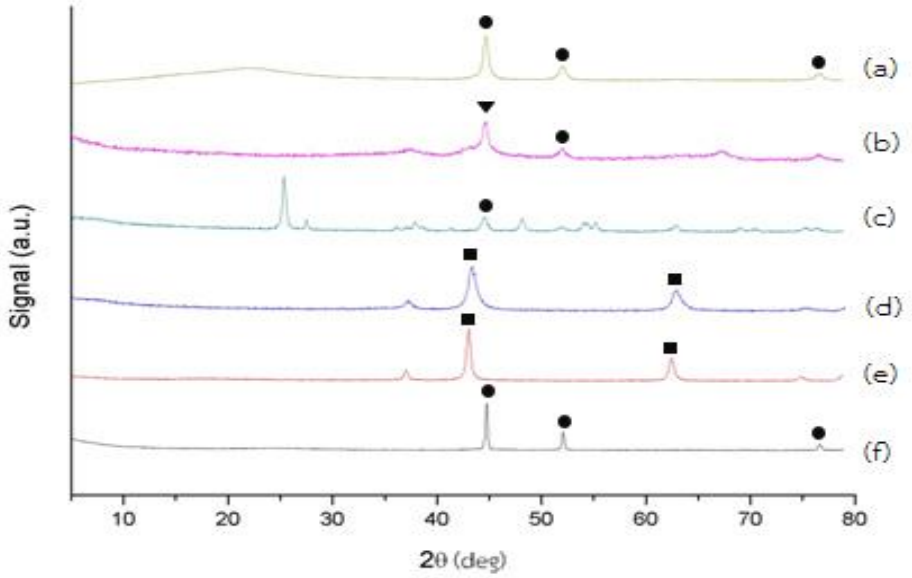

Figure 4.4 XRD patterns of (a) Ni/SiO_2, (b) Ni/Al_2O_3, (c) Ni/TiO_2, (d) Ni/LDH, (e) Ni/MgO, and (f) Ni/C (● : Ni, ▼ : Ni_2Al_3, ■ : NiO)

Ni/SiO_2 shows a broad peak at 2θ around 22°, which is attributed to amorphous silica. Ni/Al_2O_3 shows the peaks of crystalline Al_2O_3 at 37.5° and 68.4°. Ni/TiO_2 exhibits the crystalline peaks of TiO_2 at 24.5°, 26.5°, 37.3°, 38.2°, 49.5°, 53.4°, 54.5° and 63.8°. Ni/LDH shows the crystalline peaks at 37.5°, 75.5° and 79.8°. Ni/MgO shows the crystalline peaks at 37.5°, 75.5° and 79.8°. Ni/Activated carbon show a broad peak at around 15°, which is attributed to amorphous carbon. In addition, all catalysts showed the diffraction peaks of Ni at 45.5°, 52.5°, 72.5° for Ni/SiO_2, at 37.5°, 45.5°, 66.4°, 72.5° for Ni/Al_2O_3, at 24.5°, 26.5°, 37.3 °, 38.2°, 45.5°, 49.5°, 53.4°, 54.5°, 63.8°, 72.5° for Ni/TiO_2, at 37.5°, 44.7°, 63.7°, 75.5°, 79.8 ° for NiO/LDH, at 37.5°, 42.7°, 63.7°, 75.5°, 79.8 ° for NiO/MgO and at 46.5°, 52.5°, 76.8° for Ni/C. In addition, the intensity of these diffraction peaks describes the crystallinity of metal oxide phase. The high intensity reviews the larger crystallite size of nickel. This suggests the weak interaction between nickel and silica support. It is clear that the intensity of nickel diffraction peak (2θ = 45.5 °) is in this order: $Ni/SiO_2 > Ni/Al_2O_3 > Ni/TiO_2$ catalyst. Accordingly, the nickel dispersion should be in the order of: $Ni/TiO_2 > Ni/Al_2O_3 > Ni/SiO_2$.

4.2 Catalytic testing

4.2.1 Dehydration of glycerol to acrolein

Glycerol contains two different hydroxyl groups. The dehydration typically takes place at either secondary or primary hydroxyl group. It is found that the dehydrated product from secondary hydroxyl group is acrolein [2]. In a parallel dehydration at primary group, hydroxyacetone and acetaldehyde will be obtained. Acrolein is a major product from dehydration reaction over Brönsted acid catalyst, such as zeolite, in which 3-hydroxypropioaldehyde (3-HPA) is an intermediate. Due to stability and storage transportation problems, acrolein should be promptly converted to higher value chemicals after its formations. In this work, subsequently hydrogenation of acrolein to 1-propanol is attempted. The dehydration of glycerol is primarily studied using ZSM-5 zeolite (Si/Al ratio=12.5) as a catalyst at 300°C and ambient pressure. A complete conversion was obtained at contact time of 177 g.h/mol as shown in Table 4.2.

Table 4.2 The products selectivity with 100% conversion of glycerol dehydration over H-ZSM-5 (12.5)

Products	% Selectivity
Acrolein	80.0
Hydroxyacetone	15.1
1,2-propanediol	1.2
Propionaldehyde	2.5
Acetaldehyde	1.2

Reaction conditions; temperature: 300°C, feed: 1.575 g/h of glycerol at 10 wt%, ambient pressure, 100 mL/min of hydrogen

From Table 4.2 acrolein is found as a major product (80%) from dehydration at secondary hydroxyl groups; while, hydroxyacetone (15.1%) can be generated from dehydration at primary hydroxyl groups [2]. In addition, other products (5.9%) were obtained from decomposition of the feed as shown below in Figure 4.5.

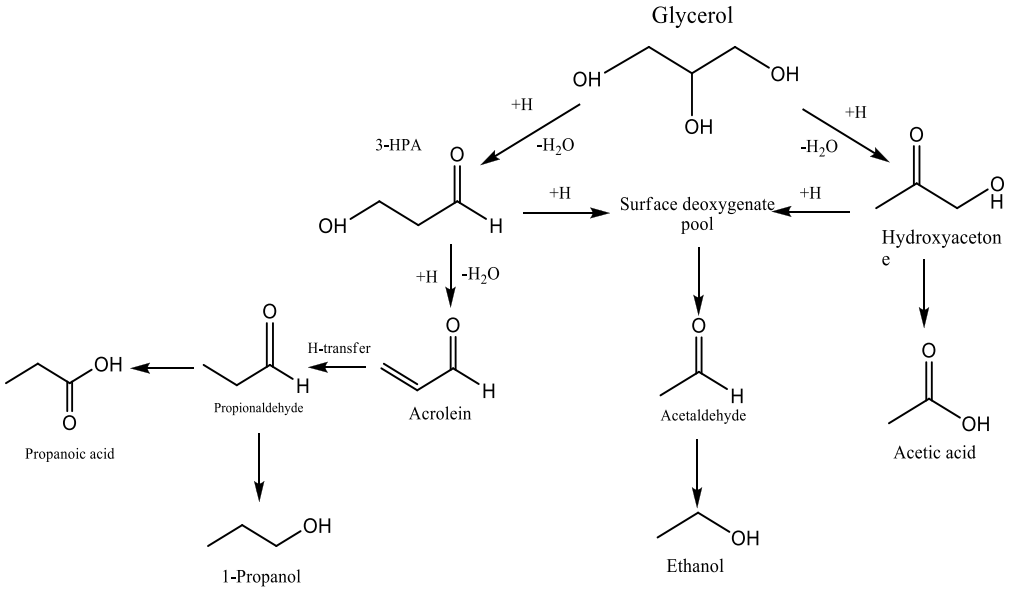

Figure 4.5 Products from glycerol dehydration reaction [2]

4.2.2 Subsequent dehydration-hydrogenation of glycerol to 1-propanol

From the optimum condition for glycerol dehydration obtained in 4.2.1, a subsequent bed of hydrogenation catalyst was added next into the reactor in order to convert the dehydrated product to 1-propanol. The Ni loaded on different supports as a second bed of reactor is tested to understand effect of supports and mechanism for 1-propanol production.

4.2.2.1 Effect of supports

The hydrogenation of acrolein from glycerol dehydration over different Ni supported catalysts was carried out at 175°C and ambient pressure. The results are shown in Table 4.3.

Table 4.3 Conversion and products selectivity obtained from subsequent dehydration-hydrogenation of glycerol

Products	Catalyst					
	Ni/Al_2O_3	Ni/TiO_2	Ni/LDH	Ni/SiO_2	Ni/MgO	Ni/C
% Conversion (based on %yield from the upper bed)						
Acrolein	99.2	98.9	98.8	98.6	77.2	64.1
Hydroxyacetone	93.1	63.7	61.5	60.1	62.7	47.9
% Selectivity (based on glycerol)						
1-Propanol	71.0	57.0	54.9	53.1	27.5	0
Propionaldehyde	7.0	18.4	22.3	22.9	44.3	67.0
Propanoic acid	2.00	4.7	2.9	4.0	8.2	13.0
Acetaldehyde	2.6	3.2	5.5	0	8.6	10.4
Ethanol	12.7	6.0	8.4	8.9	3.8	0
Acetic acid	4.7	10.8	6.2	11.1	7.6	9.6

Reaction conditions; temperature: 175°C, ambient pressure, feed: 1.575 g/h of glycerol, 100 mL/min hydrogen

The results show that a major product of two-bed reaction is 1-propanol for all supports, except MgO and activated carbon. Conversion of acrolein is calculated based on yield of acrolein that obtained from the 1st bed (80%). Selectivity of hydrogenated products is based on glycerol conversion. In addition, propionaldehyde, propanoic acid, acetic acid, acetaldehyde and ethanol are observed. Nearly 100% conversion is obtained from Ni/Al_2O_3 (99.2%), Ni/TiO_2 (98.9%), Ni/LDH (98.8%), and Ni/SiO_2 (98.6%); however, Ni/MgO and Ni/C give lower conversion as 77.2% and 64.1%, respectively. In addition, it is found that Ni/Al_2O_3 provided high selectivity to 1-propanol (71.0%), while Ni/TiO_2, Ni/LDH, and Ni/SiO_2 give lower selectivity to 57.0%, 54.9%, and 53.1%, respectively. Ni/MgO gives low selectivity (27.5%) but no 1-propanol could be obtained over Ni/C.

Considering 1-propanol production, acrolein from dehydration reaction is hydrogenated to propionaldehyde and subsequent hydrogenation to 1-propanol,

respectively. It can be seen that Ni/Al_2O_3, Ni/TiO_2, Ni/LDH, and Ni/SiO_2 has similar activity, but selectivity to 1-propanol over Ni/Al_2O_3 is likely higher than others.

The high activity and selectivity of 1-propanol over Ni/Al_2O_3 catalyst is due to the high dispersion of Ni as seen in Figure 4.6.

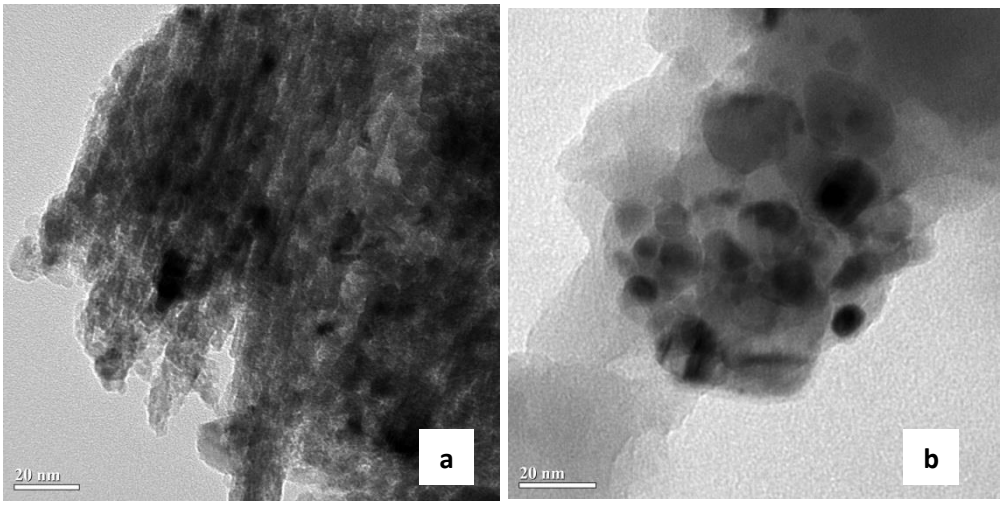

Figure 4.6 (a) TEM image of Ni/Al_2O_3 and, (b) Ni/SiO_2 catalyst

It can be seen that Ni/Al_2O_3 has small particle size than Ni/SiO_2, hence Ni/Al_2O_3 has high dispersion of metal surface compared with Ni/SiO_2. In line with the observed, Ni particle size in Ni/Al_2O_3 with low temperature reduction is observed for this catalyst (Figure 4.1). Additionally, this could be confirmed by XRD results as shown in Figure 4.4. The high intensity of nickel phase over SiO_2 reviews the larger crystallite size. This suggests the weak interaction of nickel over silica support. Accordingly, Ni particles are highly dispersed on the SiO_2 support. Due to propionaldehyde favor to adsorb over Ni/Al_2O_3 catalyst than 1-propanol, the hydrogenation to 1-propanol was preferred.

However, the 1-propanol which is subsequently hydrogenated product is also favored to adsorb over Ni/TiO_2, Ni/LDH, and Ni/SiO_2 catalysts. Accordingly, 1-propanol might be dehydrogenated back to propionaldehyde lowering the selectivity of 1-propanol as observed.

The high activity of Ni/TiO_2 catalyst can be ascribed by the strong metal support interaction effects (SMSI) [29] between Ni and TiO_2 support. Although, Ni/SiO_2 possesses weak interaction between metal and support (Figure 4.6), it is shown a high surface area

that may lead to the high activity. Since LDH contain Al-O-Mg layers that is similarly to alumina and MgO supports. It is suggested that appropriate high selectivity of 1-propanol over Ni/LDH comes from Ni disperse on alumina phase.

In contrast, Ni/MgO possesses low surface area and low interaction between metal and support [29]. Accordingly, it gives the low activity of 1-propanol production. Activated carbon support, which has poor dispersion of metal, can activate only acrolein to propionaldehyde. However, the hydrophobicity of carbon support is suppressed the hydrogenation of propionaldehyde to 1-propanol.

4.2.2.2 Effect of contact time on the second bed

In order to understand the reaction path way for 1-propanol formation by subsequent hydrogenation of acrolein from glycerol dehydration in the upper bed, Ni/SiO_2 and Ni/Al_2O_3 are tested at various contact times.The results are shown in Figure 4.7.

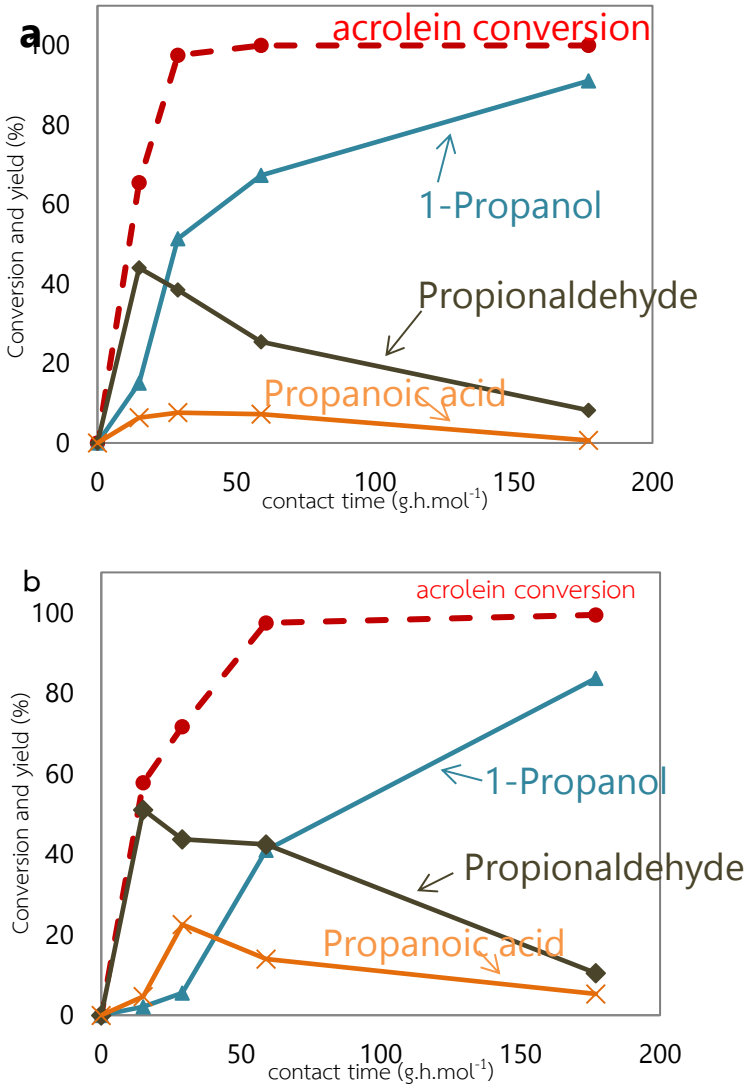

Figure 4.7 The conversion and product yields from subsequent hydrogenation of acrolein from glycerol dehydration as a function of contact time over (a) 20 wt.% Ni/Al_2O_3 (b) 20 wt.% Ni/SiO_2

Reaction condition; 1st bed: temperature: 300°C, contact time: 177 g.h/mol, catalyst: H-ZSM-5 (12.5), 2nd bed: temperature: 175°C, ambient pressure, contact time: 15–177 g.h/mol, feed: 1.575 g/h of glycerol at 10 wt.%, 100 mL/min hydrogen.

According to Figure 4.6, acrolein conversion is significantly improved as increasing the contact time and remained constantly nearly 100% conversion at more than 29 and 59 for Ni/Al_2O_3 and Ni/SiO_2, respectively. As contact time is increased, the overall interaction of reactant with active sites of supported Ni catalyst is enhanced. At low contact time, acrolein which is a dehydrated product can be primarily hydrogenated to propionaldehyde

over both Ni/Al_2O_3 and Ni/SiO_2 (Figure 4.7 (a) and (b)). When contact time is increased, propionaldehyde is decreased; while, 1-propanol is increasingly observed. It is clear that propionaldehyde will be subsequently hydrogenated to 1-propanol as observed when contact time is increased.

On Ni surface, the C=C bond of acrolein is preferentially adsorbed and hydrogenated to propionaldehyde. This intermediate can be (i) desorbed as products at low contact time or (ii) subsequently hydrogenated at carbonyl groups (C=O) to 1-propanol at high contact time (Figure 4.8).

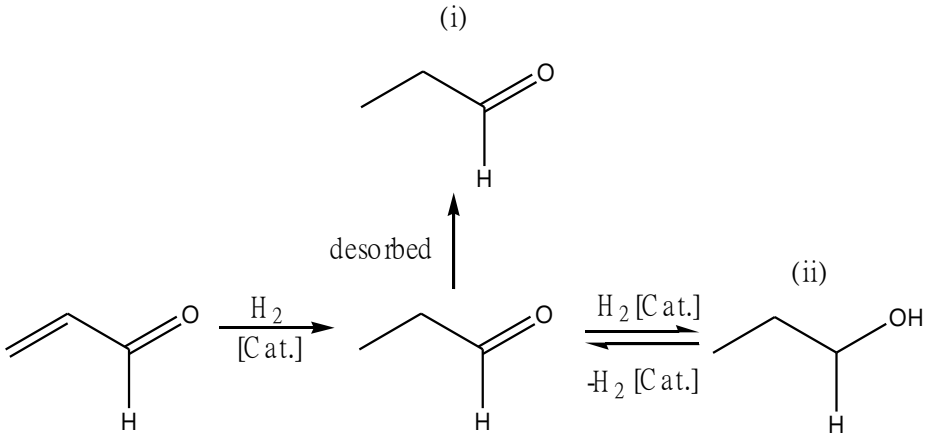

Figure 4.8 The 1-propanol production from glycerol dehydrated product

It is noted that propanoic acid is also found as a minor product being generated in parallel with the hydrogenation reaction at low contact time.

It is possible that propanoic acid can be formed by water reduction. Since water is largely presence in the reaction stream. Water may react with propionaldehyde on catalyst surface to form 1,1-propanediol, which can be dehydrogenated over Ni surface to propanoic acid as shown in Figure 4.9.

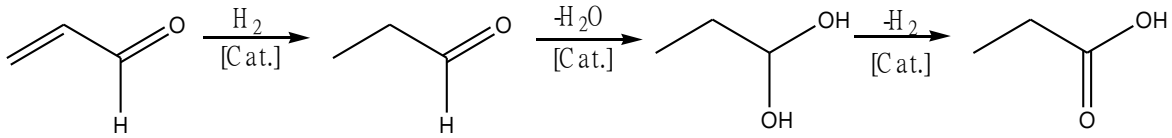

Figure 4.9 The propanoic acid formation

If this is the case, the reaction of propionaldehyde without hydrogen should give more propanoic acid. Hence, 5% propionaldehyde in water is fed over Ni/SiO_2 catalyst under nitrogen. The result is shown in Figure 4.10.

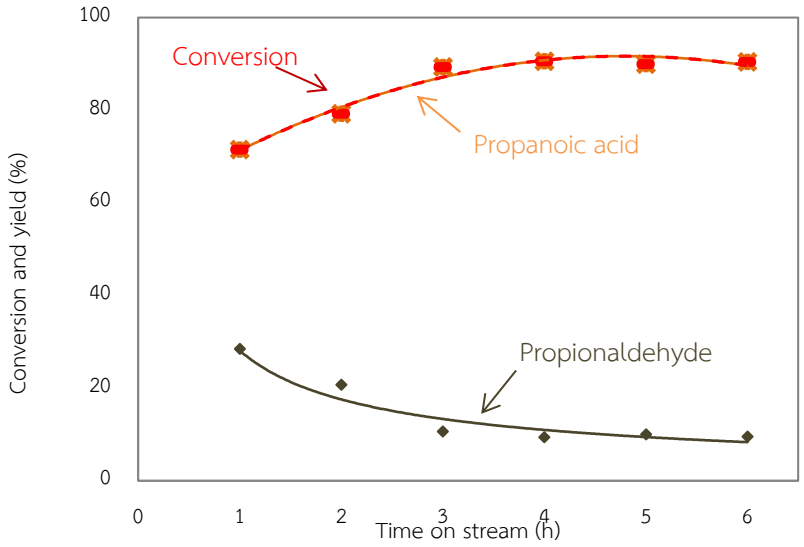

Figure 4.10 The yield of propanoic acid over time on stream of the reaction

Reaction condition; temperature: 175°C, ambient pressure, contact time: 177 g.h/mol, catalyst: Ni/SiO_2, feed: 1.575 gmol/h of propionaldehyde at 5 wt.% , 100 mL/min nitrogen

From Figure 4.10 it can be seen that only propanoic acid is produced when feeding 5% propionaldehyde in water. Therefore, this confirms that the observed propanoic acid formation is the result of the reaction between propionaldehyde and water forming 1,1-propanediol, which is subsequently dehydrogenated over Ni catalyst as discussed (Figure 4.9). Since in the subsequent dehydration-hydrogenation, H_2 is present. Therefore, yield of propanoic acid is relatively less as compared to the reaction in nitrogen.

Hence, the overall reaction in the lower bed can be summarized as following: (i) propionaldehyde is occurred from hydrogenation at C=C of acolein then desorbed as a product, (ii) 1-propanol is produced from subsequently hydrogenation of propionaldehyde at carbonyl group (C=O) and (iii) propanoic acid formation by reaction of water with propionaldehyde and subsequently hydrogenation. In addition, propanoic acid can be hydrogenated and 1-propanol is obtained [28] (Figure 4.11).

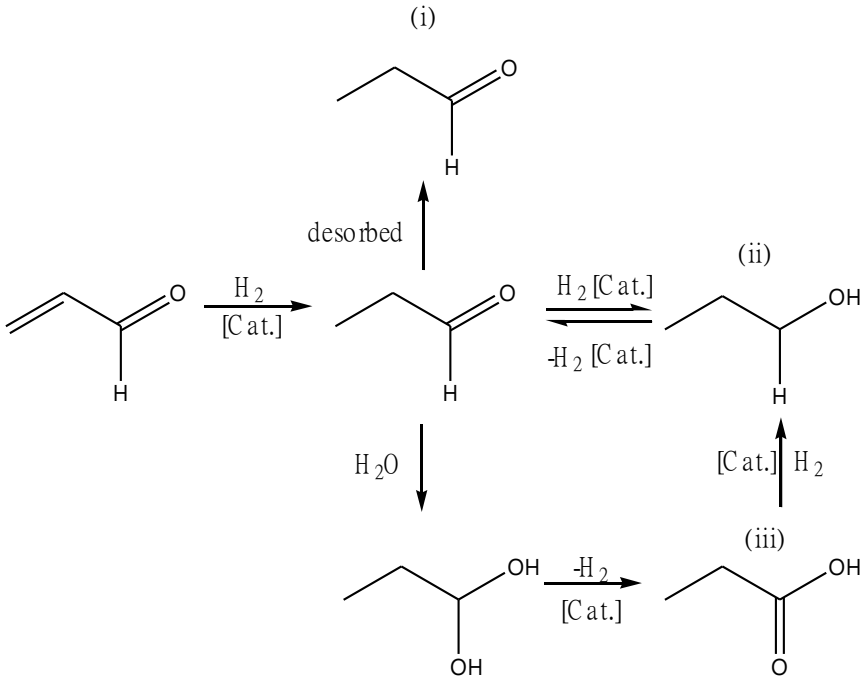

Figure 4.11 The propanoic acid production from water reduction of propionaldehyde

It is expected that Ni/Al_2O_3 promote hydrogenation of propionaldehyde to 1-propanol more effectively as compared to Ni/SiO_2 (Figure 4.7). At the low contact time (15–29 g.h/mol), acrolein is remained in the reaction steam due to an incomplete conversion over both Ni/Al_2O_3 and Ni/SiO_2. However, at this condition 1-propanol can only be produced over Ni/Al_2O_3. This is because propionaldehyde can competitively adsorb against acrolein over Ni/Al_2O_3. Hence, propionaldehyde can be further hydrogenated to 1-propanol. However, only acrolein can be adsorbed and hydrogenated to propionaldehyde, which is desorbed as a product over Ni/SiO_2.

Propionaldehyde is only produced at low contact time over Ni/SiO_2. Propionaldehyde which is occurred in the system may have a chance to react with the water and subsequent dehydrogenated to propanoic acid as well over Ni/SiO_2. While propionaldehyde can be hydrogenated to 1-propanol, the propanoic acid formation takes a few chances to be occurred over Ni/Al_2O_3. As the explanation, propanoic acid production over Ni/Al_2O_3 is less than Ni/SiO_2.

4.2.2.3 Effect of reaction temperatures

Due to hydrogenation reaction is favorable at low temperature, the effect of reaction temperature on subsequent hydrogenation of acrolein from glycerol dehydration to 1-propanol is investigated over Ni/SiO_2 as shown in Figure 4.12.

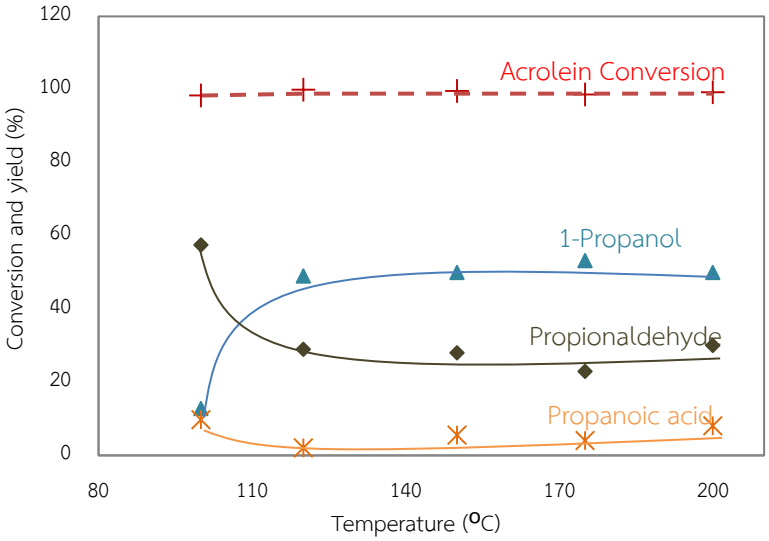

Figure 4.12 The effect of reaction temperature on acrolein conversion as a function of time on stream

Reaction condition; 1st bed: temperature: 300°C, contact time: 177 g.h/mol, catalyst: H-ZSM-5 (12.5), 2nd bed: temperature: 100–200°C, ambient pressure, contact time: 177 g.h/mol, catalyst: Ni/SiO_2, feed: 1.575 g/h of glycerol at 10 wt.%, 100 mL/min hydrogen

The results show that a complete conversion is obtained at temperatures >120°C. At low temperature (100°C), propionaldehyde is found as a main product. This is because only C=C of acrolein from glycerol dehydration can be readily hydrogenated but the hydrogenation at carbonyl group (C=O) of propionaldehyde requires higher activation energy. Therefore, low yield of 1-propanol is obtained at 100°C.

As the temperature is increased (120–200°C), it is noticed that the yield of 1-propanol and propionaldehyde is similar for all tested temperatures. This is because 1-propanol produced from propionaldehyde can adsorb on the Ni surface. Hence, dehydrogenation back to propionaldehyde could be expected over large Ni particle (Figure

4.6). Accordingly, the yield of propionaldehyde and 1-propanol is not significantly change at temperature of 120–200°C. The water reduction to produce propanoic acid seems not to be affected by temperature.

However, at the temperature higher than 200°C, the yields toward hydrogenated products are dramatically decreased, despite the conversion still being completed. This results from the decarbonylation of acrolein and propionaldehyde to ethylene and carbon monoxides is promoted at high temperatures. These gas products cannot be trapped. Hence, no product can be observed in the liquid collected at temperature >200°C. The overall reaction pathway for the hydrogenation of acrolein from glycerol dehydration is shown in Figure 4.13.

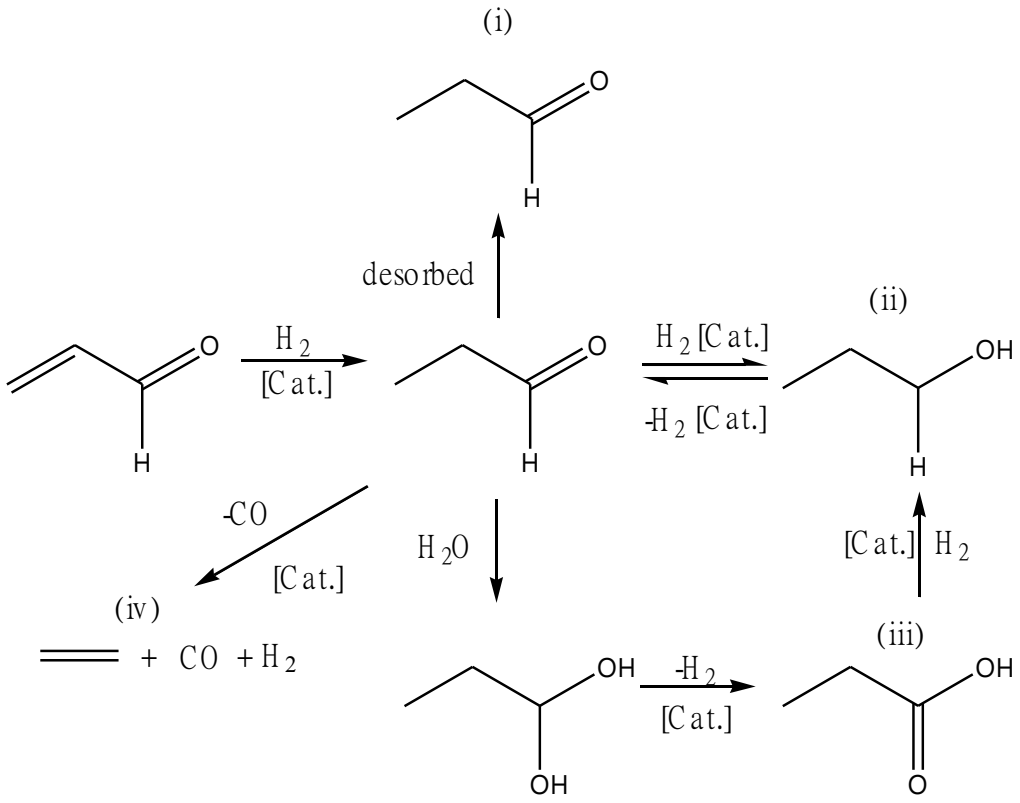

Figure 4.13 The pathway for hydrogenation of acrolein from glycerol dehydration

4.2.2.4 Catalytic deactivation

From the previous result, all catalysts seem to show deactivation particularly for Ni/SiO_2. Accordingly, the effect of time on stream at reaction temperature of 175°C for the conversion of acrolein from glycerol dehydration is studied as shown in Figure 4.14.

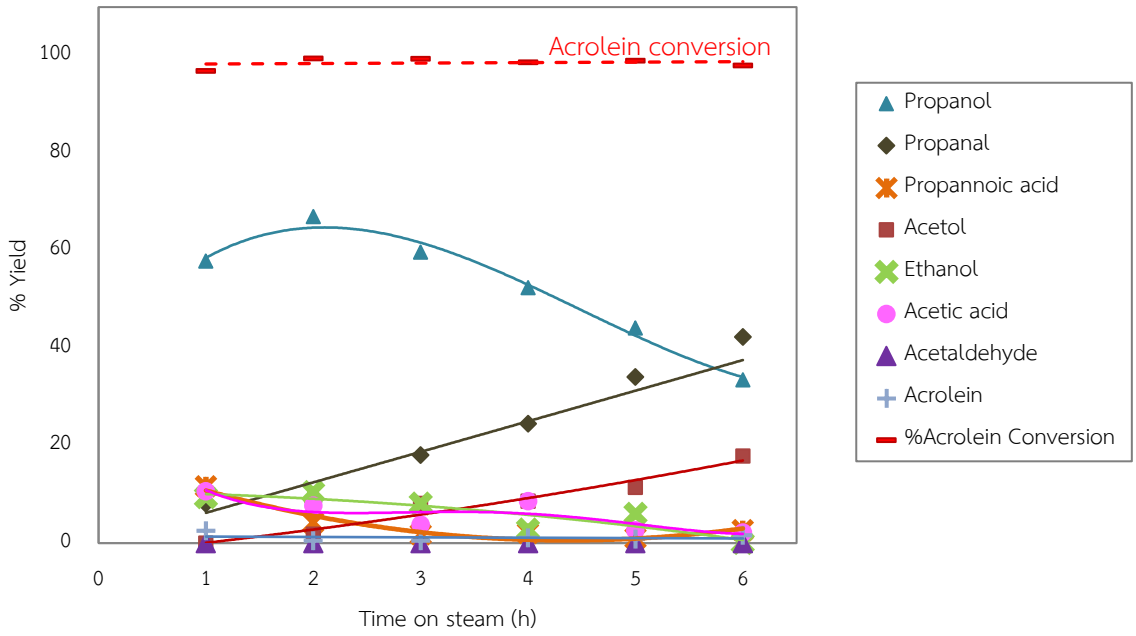

Figure 4.14 The conversion of acrolein from glycerol dehydration

Reaction condition; 1st bed: temperature: 300°C, contact time: 177 g.h/mol, catalyst: H-ZSM-5 (12.5), 2nd bed: temperature: 175°C, contact time: 177 g.h/mol, catalyst: Ni/SiO_2 feed: 1.575 g/h of glycerol at 10 wt.%, ambient pressure, 100 mL/min of hydrogen

From Figure 4.14, despite acrolein being virtually hydrogenated, 1-propanol production is decreased with time on steam. This suggests that the catalyst was deactivated to produce 1-propanol all the time. The catalyst deactivation is possible due to (i) leaching of metal function, (ii) sintering of metal, (iii) strong adsorption of reactant, (iv) strong adsorption of product or (v) deposition of high molecular weight product over catalyst.

It is possible that propanoic acid formed as a minor product can be the cause of metal leaching. This is because nickel metal is weakly interacted with silica support and propanoic acid could be corrosive for Ni. Accordingly, the amount of nickel on silica support before and after reaction is checked as shown in Table 4.4.

Table 4.4 Ni content in fresh and spent Ni/SiO_2 catalyst

Catalyst	% Nickel loading
Fresh Ni/SiO_2	22.7
Used Ni/SiO_2	22.3

From Table 4.4, %Ni of fresh and used Ni/SiO_2 catalyst remained the same. The amount of nickel on silica support did not change after the reaction. Accordingly, metal leaching is not the cause of catalyst deactivation.

Alternatively, the catalyst sintering along the reaction may take place and the dispersion of nickel metal over the support surface is decreased. This could reduce the active metal surface and observe the deactivation. The sintering of nickel over support was investigated by TEM as presented in Figure 4.15.

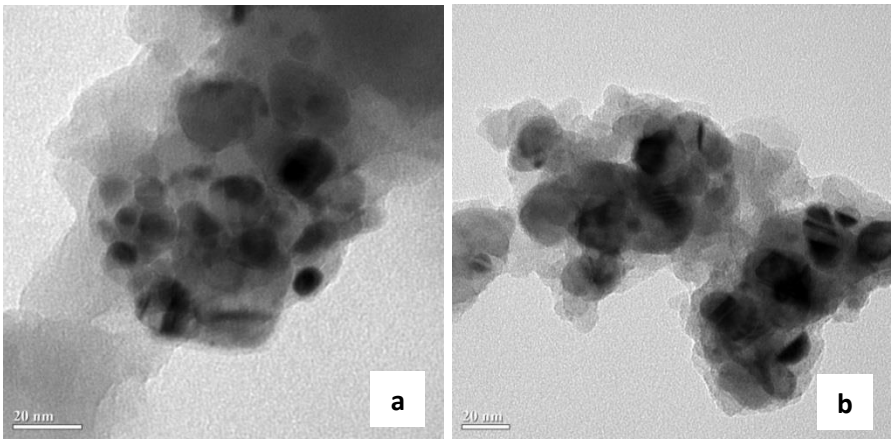

Figure 4.15 TEM image of (a) fresh, (b) used Ni/SiO_2 catalysts

According to the TEM images in Figure 4.15, the dispersion of Ni on the fresh and used Ni/SiO_2 catalyst is unchanged. The dispersion of Ni/SiO_2 still remains the same. Hence, it can be summarized that sintering should not be the cause of catalyst deactivation.

One could expect that the strong adsorption of reactant could be the cause of deactivation. This can be verified by removing reactant from the reaction while running.

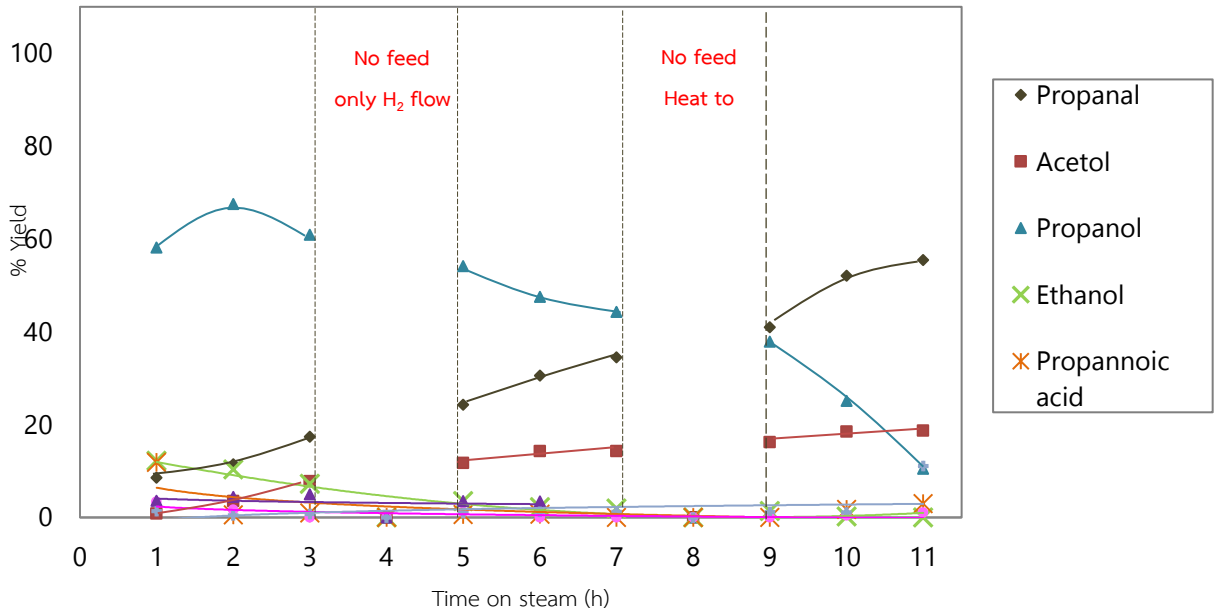

Figure 4.16 Deactivation test

Reaction condition; 1st bed: temperature: 300°C, contact time: 177 g.h/mol, catalyst: H-ZSM-5 (12.5), 2nd bed: temperature: 175°C, ambient pressure, contact time: 177 g.h/mol, catalyst: Ni/SiO_2, feed: 1.575 g/h of glycerol at 10 wt.%, 100 mL/min hydrogen.

The investigation is started by feeding acrolein for 3 hours. Then at the 4th hour of time on stream, the feed has been paused; only an excess amount of hydrogen is fed in the system. After the system is filled of hydrogen for 1 hour, the feed is then re-introduced at the 5th hour of time on stream to study the tendency of the overall reaction. It is found that the yield of 1-propanol is continuously decreased, whereas, the yield of propionaldehyde is increased. It can be suggested that stop feeding is ineffective to reactivate the catalyst. It is suspected that the feed may still adsorb on catalyst surface. Hence, the feed has been stopped again at 8th hour on stream the lower bed then heat to 300°C and held for an hour under H_2 flow (the temperature in the upper bed is fixed at 300°C). After cooled down to the reaction temperature of 175°C the glycerol is then fed again at 10th hour on stream. The result shows that the yield of propanol is still decreased steadily, whereas, the yield of propionaldehyde is also increased. Following the same trend as previously observed. If the adsorption of reactant is a cause of deactivation, it is not possible that the reactant cannot be desorbed at 300°C. Thereafter, acrolein did not have a strong adsorption with catalyst that lead to the catalyst deactivation.

As all above hypotheses are not the case for deactivation, it is possible that the strong adsorption of products either propionaldehyde or hydroxyacetone may lead to catalyst deactivation. This can be verified by feeding propionaldehyde and propionaldehyde /hydroxyacetone mixtures over Ni/SiO_2 catalyst and the result is shown in Figure 4.16.

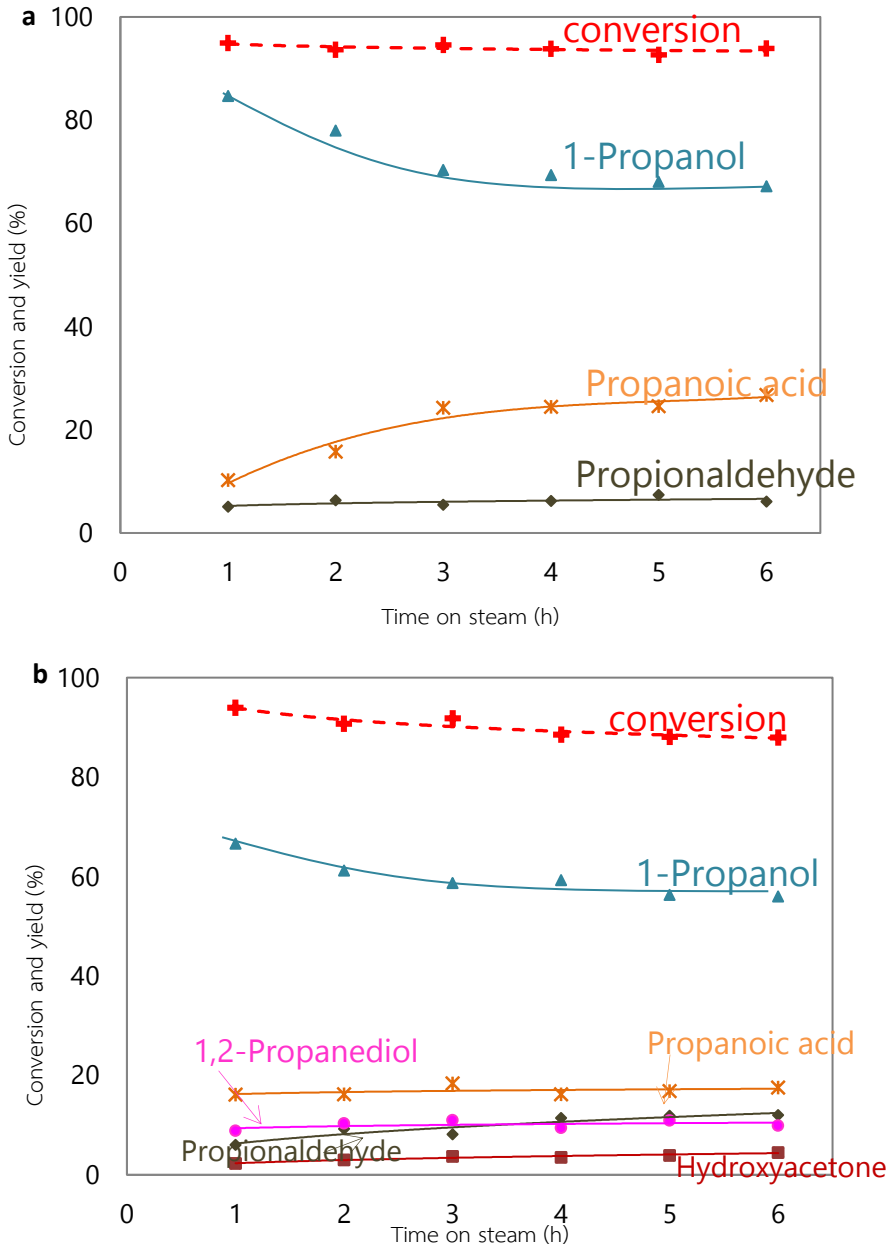

Figure 4.17 The conversion and yield over Ni/SiO_2 as a function of time on stream using (a) 5 wt.% propionaldehyde (b) 5 wt.% propionaldehyde/1.6 wt.% hydroxyacetone as feed

As seen in Figure 4.17 (a) and (b), propionaldehyde are completely converted to 1-propanol and propanoic acid via hydrogenation and water reduction (Figure 4.7 (a)); while, 1,2-propanediol is a hydrogenated product of hydroxyacetone. No deactivation due to hydrogenation activity can be observe. Therefore, with H_2-enriched system, strong adsorption of products is not the cause of catalyst deactivation.

Alternatively, it is possible that the deposition of high molecular weight product over catalyst could be the cause of the catalyst deactivation. This can be verified by TGA as the result shown in Table 4.5.

Table 4.5 Percentage of weight loss in spent Ni/SiO_2 and Ni/Al_2O_3 catalysts. (after 6 h time on stream)

Catalyst	**%wt. loss (300–400°C)**
Ni/SiO_2	7.43
Ni/Al_2O_3	6.30

TGA Condition: 10 °C /min in air from 50°C to 900°C.

. From Table 4.5, it can be seen that both Ni/SiO_2 and Ni/Al_2O_3 shows significantly high %weigh loss at 300–400°C. It is noted that higher molecular weight species or coke are deposited on the surface of the catalysts, leading to a significant decreasing of 1-propanol yield over time on stream. Hence, it can be suggested that deposition of a high molecular product over catalyst should be the cause of catalyst deactivation. The fact that Ni/Al_2O_3 show a higher stability as compare to Ni/SiO_2, is presumably the higher dispersion of metallic Ni on the support (Figure 4.6).

บทที่ 5

สรุปผลการวิจัยและข้อเสนอแนะ

5.1 Conclusions

The catalytic deoxygenation of glycerol to 1-propanol was studied using sequential bed system. In the upper bed, H-ZSM-5 (Si/Al=12.5) is used as a catalyst for dehydration of glycerol. Acolein and hydroxyacetone is a major and minor product, respectively. In the lower bed, supported Ni catalysts are used for subsequently hydrogenation of acrolein to 1-propanol. It was found that propionaldehyde is an important intermediate to produce the major product 1-propanol via hydrogenation, while propanoic acid is a minor product obtained from water reduction. Interaction between metal and support significantly affects the hydrogenation activity and yield of 1-propanol in the lower catalytic bed. The orders of hydrogenation activity of supported Ni catalysts are as following: Ni/Al_2O_3 > Ni/TiO_2 > Ni/LDH > Ni/SiO_2 > Ni/MgO > Ni/C. The high activity of Ni/Al_2O_3 is due to the high Ni dispersion on the catalyst surface. The activity of Ni/TiO_2 catalyst can be also ascribed by high dispersion of Ni due to the strong metal support interaction effects (SMSI). Ni/LDH contains Al-O-Mg layers, which promotes the high dispersion of Ni on alumina phase. It is noted that activity of Ni/SiO_2 is due to its high surface area, while Ni/MgO possesses low surface area and low metal-support interaction. Ni/C presents poor Ni dispersion and hence, low activity. At low temperature (100°C), propionaldehyde is found as a main product because activation energy for C=O hydrogenation is insufficient. As the temperature is increased (120–200°C), it is noticed that yield of 1-propanol and propionaldehyde is similar for all tested temperature, presumably due to the saturated kinetics for hydrogenation-dehydrogenation over large Ni particle. However, at temperature > 200°C the decarbonylation of propionaldehyde yielding ethylene and carbon monoxides is promoted. The deactivation of catalyst is observed due to deposition of high molecular weight product on the catalysts.

5.2 Suggestions for Future Studies

5.2.1) The elimination of silanol group of H-ZSM-5 from glycerol dehydration in the first bed likely increases yield of acrolein that is major product.

5.2.2) Changing feed solvent from water to others is interested to decrease the yield of by-product propanoic acid from water reduction in second bed.

บทที่ 6

สรุปผลผลิตงานวิจัย

1. Catalytic deoxygenation of glycerol to 1-propanol over zeolite and supported Ni catalysts in sequential bed system, Thanasak Solos, Kroegchai Matee, Chanakran Homla-or, Preedawan Duangchan, Natthida Numwong, Tawan Sooknoi, PACCON 2017, Bangkok, Thailand, 2-3 February 2017

บรรณานุกรม

1. Amin, I.N.H.M. Mohammad, A.W. Markom, M. Peng, L.C. and Hila, l.N. 2010. “Analysis of deposition mechanism during ultrafiltration of glycerin-richsolutions.” *Desalination* 261 : 313–20.
2. Witsuthammakul, A. and Sooknoi, T. 2012. “Direct conversion of glycerol to acrylic acid via integrated dehydration–oxidation bed system.” *Applied Catalysis A: General* 413– 414 : 109– 116.
3. Tsukuda, E. Sato, S. Takahashi, R.i and Sodesawa, T. 2007. “Production of acrolein from glycerol over silica-supported heteropoly acids.” *Catalysis Communications* 8: 1349–1353.
4. L. Znak, J. Zielin´ski. “Effects of support on hydrogen adsorption/desorption on nickel.” *Applied Catalysis A: General* 334 (2008) 268–276.
5. Ueoka, H. and Katayama, T. 2001. **Process for preparing glycerol, United States Patent**.
6. JG. Speight, Chemical process and design handbook. United States: McGraw- Hill Professional, 2002.
7. Pagliaro, M. and Rossi, M. 2010. **Future of glycerol.** 2nd ed. London: Royal Society of Chemistry.
8. Glycerine: an overview. 1990. **The soap and detergent association**.
9. Centi, G. and Santen, R. A. van 2007. “Catalysis for renewables: from feedstock to energy production.” Weinheim: Wiley-VCH.
10. Katryniok, B. Paul, S. Bellière-Baca, V. Rey, P. and Dumeigni, F. 2010. “Glycerol dehydration to acrolein in the context of new uses of glycerol.” *Green Chem.* 12 : 2079–98.
11. Talebian-Kiakalaieh, A. Amin, N. A. S. and Hezaveh, H. 2014. “Glycerol for renewable acrolein production by catalytic dehydration.” *Renewable and Sustainable Energy Reviews* 40 : 28–59.

12. R. A. Sheldon and H. van Bekkum. 2001. *Fine Chemicals through Heterogeneous Catalysis*. 295-304.
13. Bagheri, S. Julkapli, N. Muhd and Yehye,W. A. 2015. "Catalytic conversion of biodiesel derived raw glycerol to value added products." *Rene. and Sust. Ener. Rev.* 41 : 113–127.
14. Suprun, W. Lutecki, M. Haber, T. and Helmut, Papp. 2009. "Acidic catalysts for the dehydration of glycerol: Activity and deactivation." *Journal of Molecular Catalysis A: Chemical.* 309 : 71–78.
15. de Oliveira, A. S. Vasconcelos, S. J.S. Sousa, J. R. de Sousa, F. F. Filho, de J. M. and Oliveira, A. C. 2011. "Catalytic conversion of glycerol to acrolein over modified molecular sieves: Activity and deactivation studies." *Chemical Engineering Journal* 168 : 765–774.
16. C. H. Bartholomew and Robert J. Farrauto. Fundamentals of Industrial Catalytic Processes, 2nded., John Wiley & Sons, Inc., New Jersy, 2005, 578-584, 606-609.
17. J. Hagen. 1999. **Industrial Catalysis: A Practical Approach**. 1st ed. Wiley-VCH : Weinheim. 1-11.
18. Sooknoi, T. **Zeolites and Related Microporous Materials.** 17, 50.
19. Haag, S. Hanebuth, M. Mabande, G. T.P. Avhale, A. Schwieger, W. and Dittmeyer, R. 2006. "On the use of a catalytic H-ZSM-5 membrane for xylene isomerization." *Microporous and Mesoporous Materials.* 96 : 168–176.
20. Lermer, H. Draeger, M. Steffen, J. and Unger, K.K. 1985. "Synthesis and structure refinement of ZSM‒5 single crystals." *Zeolites* ***5.*** (3): 131–134.
21. Zhou, CJ. Huang, CJ. Zhang, WG. Zhai, HS. Wu, HL. and Chao, ZS. 2007. "Synthesis of micro and mesoporous ZSM-5 composites and their catalytic application in glycerol dehydration to acrolien*." Study Surface Science Catalysis.* 165 : 527–30.
22. Hoang-Van, C. and Zegaoui, O. 1997. "Studies of high surface area Pt/MoO_3 and Pt/WO_3 catalysts for selective hydrogenation reactions. II. Reactions of acrolein and allyl alcohol". *Applied Catalysis A: General.* 164 : 91-103.

23. Peng, G. Wang, X. Chen, X. Jiang, Y. and Mu, X. 2013. "Zirconia-supported niobia catalyzed formation of propanol from 1,2-propanediol via dehydration and consecutive hydrogen transfer." *Journal of Industrial and Engineering Chemistry*
24. Hoang-Van, C. and Zegaoui, O. 1997. "Studies of high surface area Pt/MoO_3 and Pt/WO_3 catalysts for selective hydrogenation reactions. II. Reactions of acrolein and allyl alcohol." *Applied Catalysis A: General.* 164: 91-103.
25. Volckmar, C. E. Brona, M. Bentrup, U. Martin, A. and Claus, P. 2009. "Influence of the support composition on the hydrogenation of acrolein over $Ag/SiO_2–Al_2O_3$ catalysts." *Journal of Catalysis.* 261 : 1–8.
26. Nishimura, S. **Handbook of Heterogeneous Catalytic Hydrogenation for Organic Synthesis..** 1-3, 51-59, 170.
27. **Hydrogenation.** [Online]. Available : http://en.wikipedia.org/wiki/Hydrogenation.
28. Wang, Z. Li, G. Liu, X. Huang, Y. Wang, A. Chu, W. Wang, X. and Li, N. 2014. "Aqueous phase hydrogenation of acetic acid to ethanol over $Ir\text{-}MoO_x/SiO_2$ catalyst" Catalysis Communications. 43 : 38–41.
29. Busca, G. **Heterogeneous Catalytic Materials.** 131-136, 161-164, 316-320.
30. Anderson, J. A. and Garcia, M. F. **Supported Metals in Catalysis.** 71.
31. General catalyst catalogue, Sud Chemie; 2012. Available on the web.
32. Evonik, brochure. **Continuous process catalysts.** [Online]. Available: www.evonik.com
33. **Activated carbon.** [Online]. Available : http://en.wikipedia.org/wiki/Activated_carbon
34. 2006. **Activated carbon.** [Online]. Available : http://www.cameroncarbon.com/documents/ carbon_structure.pdf
35. Costentin, ML. Bailly Lauron-Pernot, G. Krafft, H. JM. and M. J. 2005. *Che. Phys Chem B* 109 : 2404e13.
36. K, A. Ghamdi SJS, H. J. SD. In. SD, Jackson and SJS, Hargreaves editors. 2009. **Metal oxide catalysis.** Wiley. pp. 819e43.
37. **Layered Double Hydroxide**. [Online]. Available : http://www.google.co.th/books?hl=th&lr&id=qujowYGyNagC&oi=fnd&pg=PA1&dq=l

ayered+double+hydroxide&ots=Ohzb6721RO&sig=jaFgKZRczYfRvW5sj7mjH4ImSY&redir_esc=y#v=onepage&q=layered%20double%20hydroxide&f=false

38. Eriksson, L. and Palmqvist, U. S. Neutron Research Laboratory Report 482**,** Copyright University of Stockholm.
39. December 12, 2013. **Porous Materials Retrieved.** [Online]. Available : http://www.uio.no/studier/emner/matnat/kjemi/KJM5100/h06/undervisningsmateriale/16KJM5100_2006_porous_e.pdf
40. S. B. Wang, and G. Q. M. Lu, 1998. *Appl. Catal. B-Environmantal.* 15 : 269.
41. G. Q. Lu, and S. B. Wang, 1999. *Chemtech.* 29 : 37.
42. Tang, S. Ji, L. Lin, J. Zeng, H. C. Tan, K. L. and Li, K. 2000. *J. Catal.* 194 : 424.
43. Bitter, J. H. Hally, W. Sechan, K. Ommen, J. G. van and Lercher, J. A. 1996. *Catal. Today* 29 : 349.
44. Ruckenstein, E. and Hu, Y. H. 1996. *J. Catal.* 162 : 230.
45. Zhang, Z. L. Tsipouriari, V. A. Efstathiou, A. M. and Verykios, X. E. 1996. *J. Catal.* 158 : 51.
46. Nakagawa, K. Anzai, K. Matsui, N. Ikenaga, N. Suzuki, T. Teng, Y. H. Kobayashi, T. and M. Haruta, 1998. *Catal. Lett.* 51 : 163.
47. Bradford, M. C. J. and Vannice, M. A. 1999. *Catal. Today* 50 : 87.
48. Chen, H. Xue, M. Hu, Shenghua and Shen, J. 2012 “The effect of surface acidic and basic properties on the hydrogenation of lauronitrile over the supported nickel catalysts.” *Chemical Engineering Journal.* 181– 182 : 677– 684.
49. December 12, 2013. **1-Propanol.** [Online]. Available: http://en.wikipedia.org/wiki/1-Propanol
50. Ryneveld, E. van Mahomed, Abdul S. Heerden, Pieter S. van Green, Mike J. and Friedrich, Holger B. 2011 “A catalytic route to lower alcohols from glycerol using Ni-supported catalysts.” *Green Chem.* 13 : 1819.

ภาคผนวก

ภาคผนวก ก

Crystalline structure analysis by X-ray diffraction

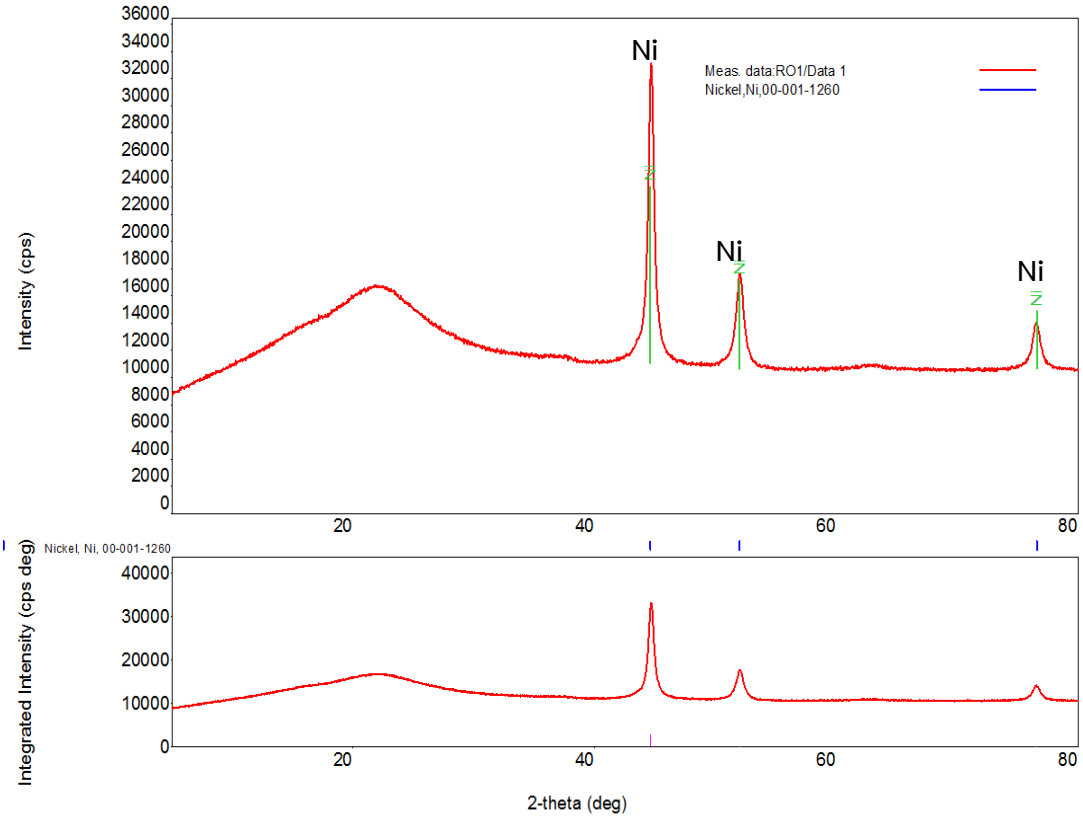

Figure A1 XRD of Ni/SiO_2

Measurement conditions: 40 kV, 30 mA, scan speed: 1.0000 deg/min, step width: 0.04 deg, scan range 5.00-80.00 deg.

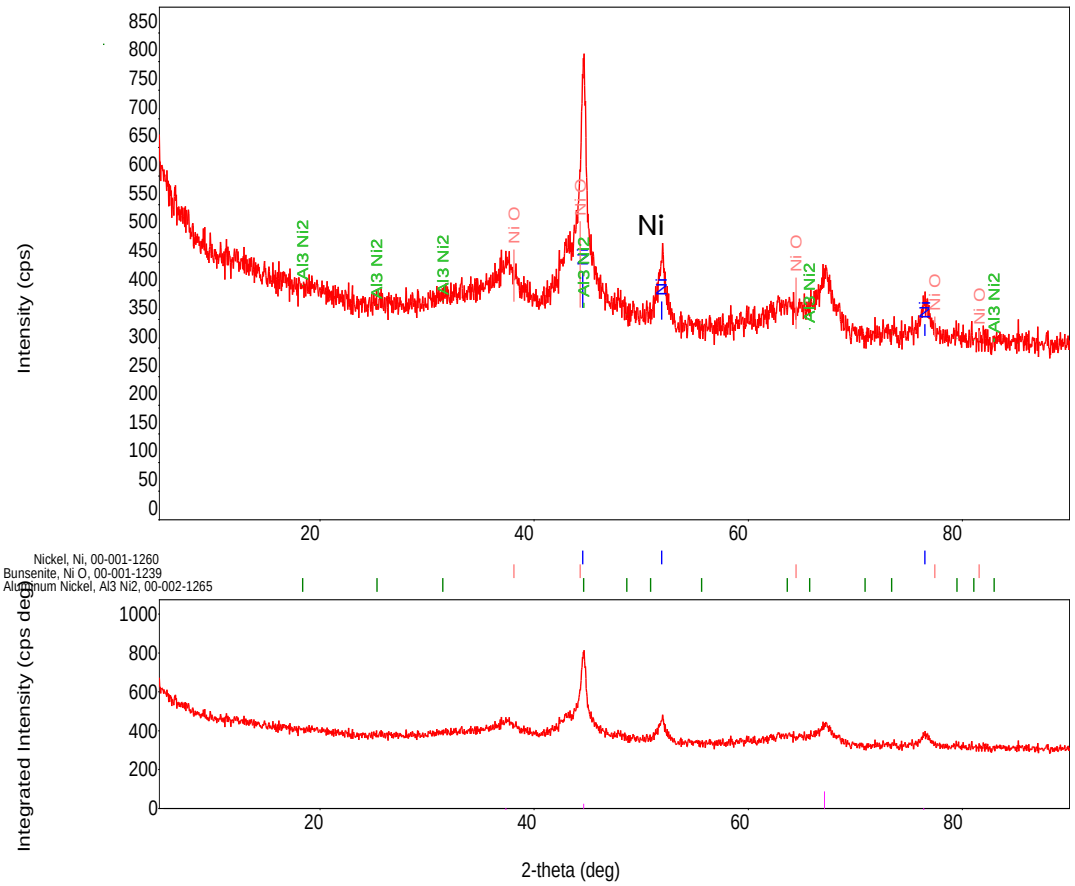

Figure A2 XRD of Ni/Al_2O_3

(Measurement conditions are same as Figure A1)

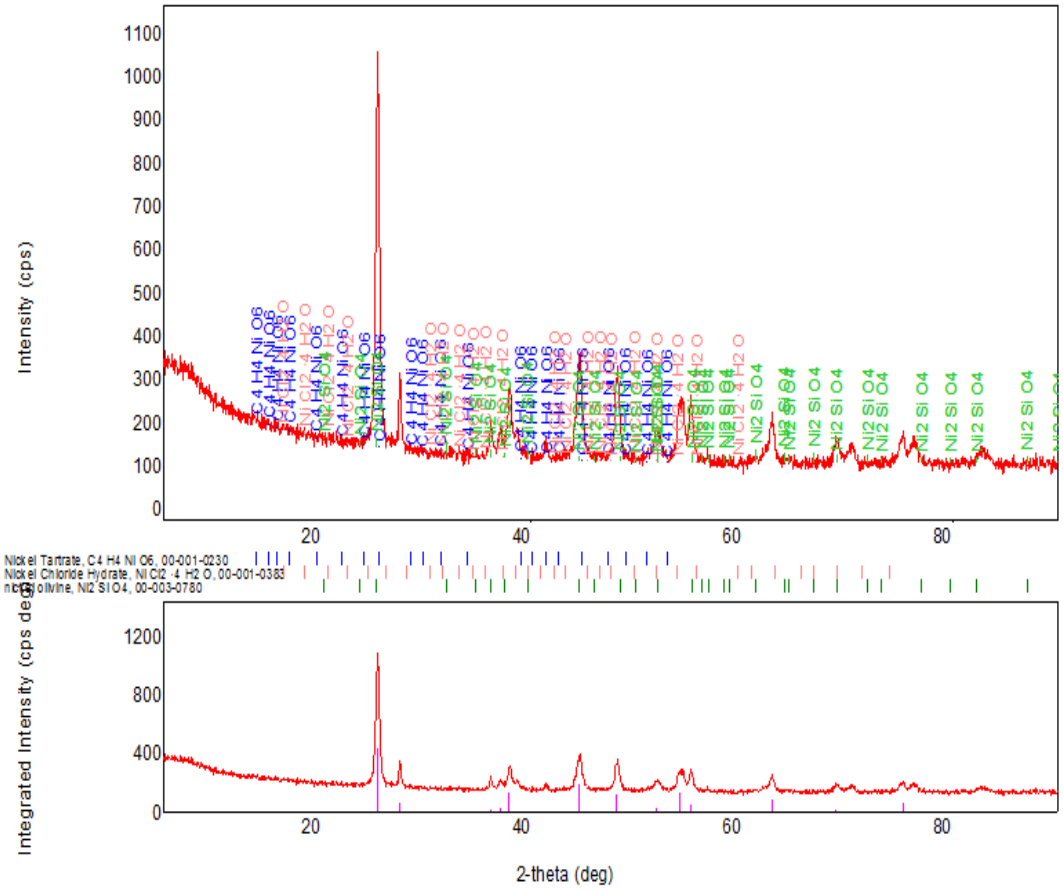

Figure A3 XRD of Ni/TiO_2

(Measurement conditions are same as Figure A1)

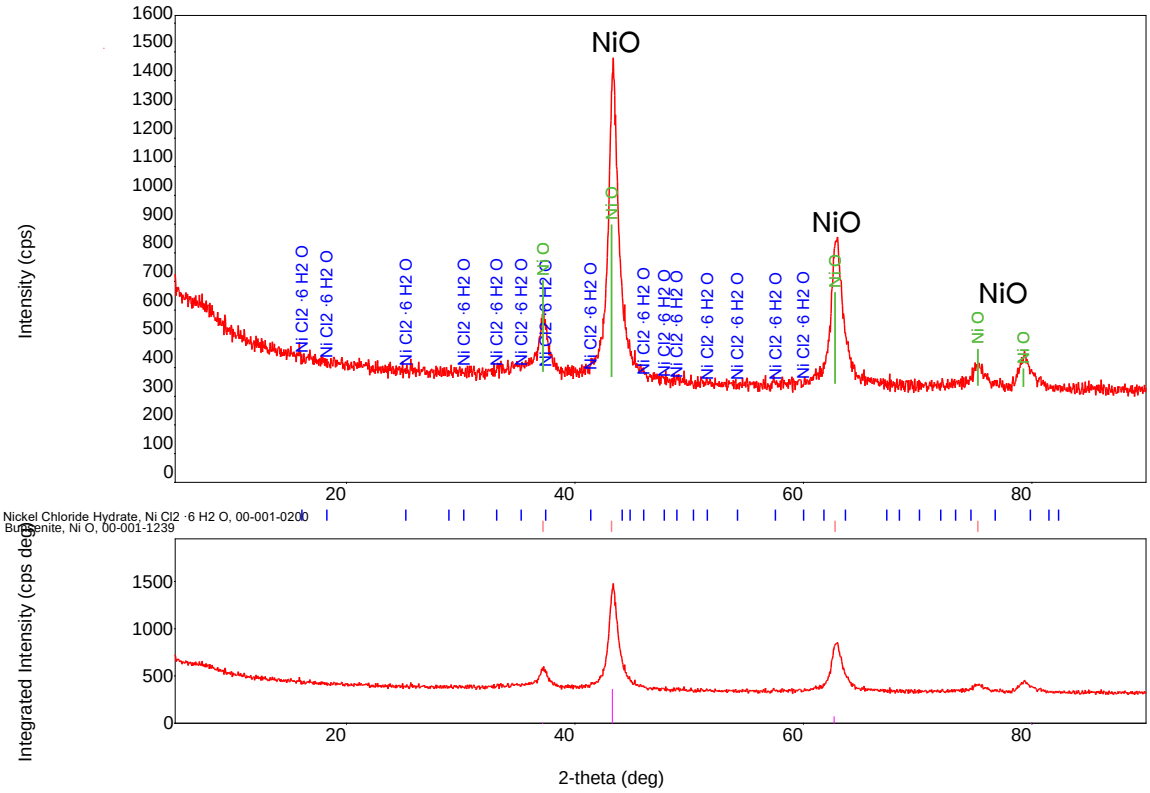

Figure A4 XRD of Ni/LDH

(Measurement conditions are same as Figure A1)

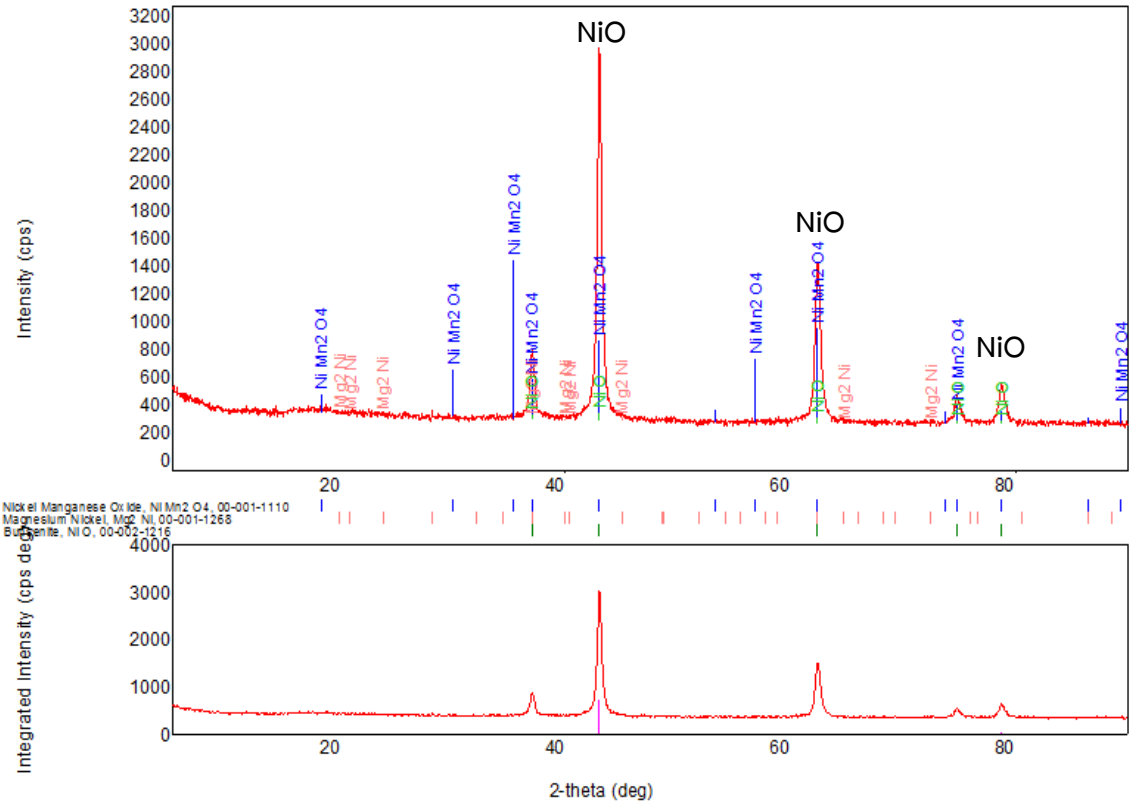

Figure A5 XRD of Ni/MgO

(Measurement conditions are same as Figure A1)

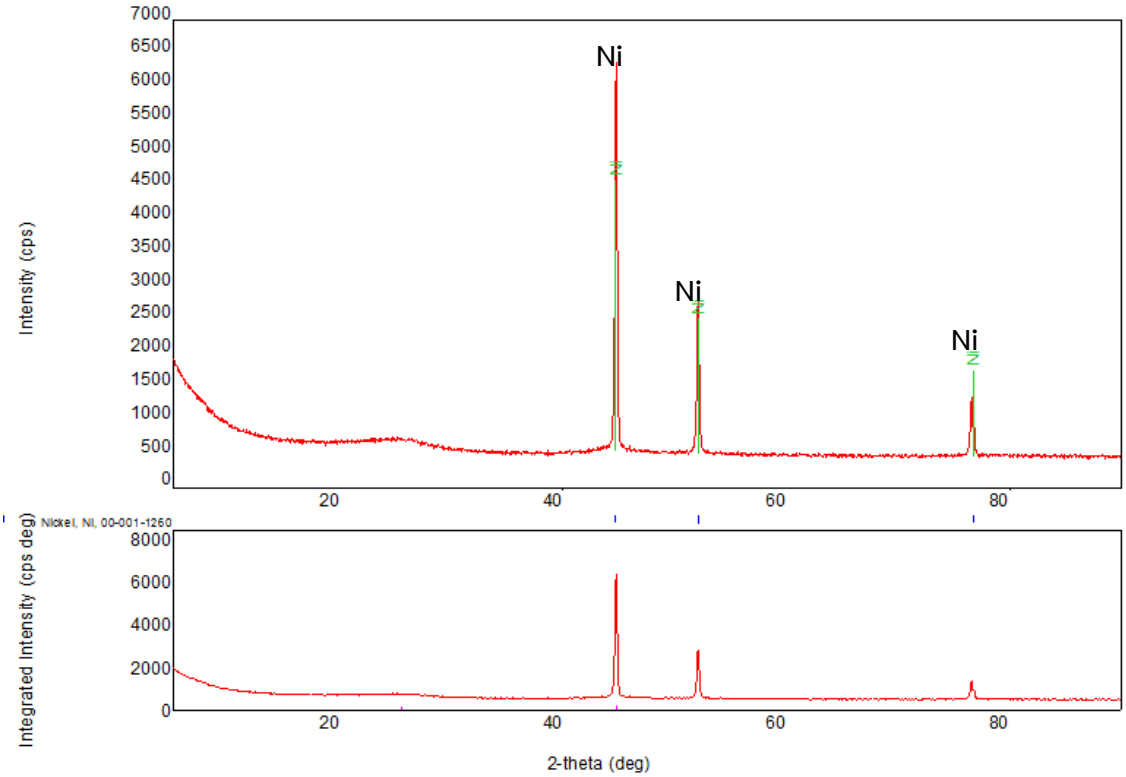

Figure A6 XRD of Ni/C

(Measurement conditions are same as Figure A1)

ภาคผนวก ข

Elemental analysis by X-ray fluorescence

Table B1 Elemental composition of 20 wt. % Ni/SiO_2 catalyst

Al_2O_3	SiO_2	NiO	CuO	Compton
0.0 KCps	45.2 KCps	355.7 KCps	3.3 KCps	9.1 KCps
666 PPM	72.4 %	26.8 %	0.191	35 %

Table B2 Elemental composition of 20 wt. % Ni/Al_2O_3 catalyst

Al_2O_3	SiO_2	Ni	MgO	Compton
40.6 KCps	0.2 KCps	352.7 KCps	1.3 KCps	14.6 KCps
67.6 %	0.384 %	22.0 %	1.49%	19 %

Table B3 Elemental composition of 20 wt. % Ni/TiO_2 catalyst

Al_2O_3	SiO_2	Ni	TiO_2	MgO	Compton
0.2 KCps	0.1 KCps	146.8 KCps	134.5 KCps	1.0 KCps	5.0 KCps
0.318 %	0.178 %	20.9 %	77.0 %	1.38 %	35 %

Table B4 Elemental composition of 20 wt. % Ni/LDH catalyst

Al_2O_3	SiO_2	NiO	MgO	Compton
8.2 KCps	0 KCps	KCps	43.6 KCps	9.0 KCps
19.6%	0	22.8 %	48.9 %	35%

Table B5 Elemental composition of 20 wt. % Ni/MgO catalyst

Al_2O_3	SiO_2	Ni	MgO	Compton
0.0 KCps	O.2 KCps	432.8 KCps	57.9 KCps	7.9 KCps
0.118%	0.443 %	22.3 %	69.6%	32%

Example of elemental composition calculation from **Table B1**

Mole of each compositions :

SiO_2 = 26.8 g / (60.080 g/mol) = 0.4461 mol

NiO = 26.8 g / (74.690 g/mol) = 0.359 mol

CuO = 0.191 g / (79.545 g/mol) = 0.002 mol

Weight of each elementals :

Si = 0.4461mol × (28 g/mol) = 12.5 g

Ni = 0.359 mol × (58.69 g/mol) = 21.2 g

Cu = 0.002mol × (63.55 g/mol) = 0.1271 g

ภาคผนวก ค

Reaction Data

E1 : Glycerol dehydration over zeolite H-ZSM-5

Table E1 The yield of glycerol dehydration at contact time = 177 g.h.mol^{-1} (H-ZSM-5 ratio 12.5).

Time on steam	Conversion	Yield (%)				
(h)	(%)	Acrolein	Propanal	Hydroxacetone	1,2-PDO	Acetaldehyde
1	100	85.6	5.7	10.0	1.1	1.4
2	100	86.1	4.5	8.0	1.3	1.3
3	100	74.8	3.1	20.5	1.6	1.5
4	100	78.0	3.3	17.6	1.1	1.1
5	100	81.6	3.5	14.1	0.7	0.7
6	100	77.9	3.1	17.5	1.5	1.5

E2 : Glycerol deoxygenation over zeolite H-ZSM-5 and 20 wt.% Ni/SiO_2, 20 wt.% Ni/Al_2O_3, 20 wt.% Ni/TiO_2, 20 wt.% Ni/LDH, 20 wt.% Ni/MgO, and 20 wt.% Ni/C

Table E2 The yield of the glycerol deoxygenation over zeolite H-ZSM-5 and 20 wt.% Ni/SiO_2 at contact time = 177 g.h.mol^{-1}

Time on steam	Conversion in 2nd bed		Yield (%)					
(h)	Acrolein	Hydroxy-acetone	1-Propanol	Propional-dehyde	Propanoic acid	Acetalde-hyde	Ethanol	Acetic acid
1	96.9	100	57.8	8.0	11.6	0	9.4	10.6
2	99.4	90.8	67.0	8.3	4.3	0	8.3	7.7
3	99.4	59.3	59.7	18.0	1.8	0	8.1	3.8
4	98.7	56.9	52.4	24.4	2.0	0	2.8	8.6
5	99.0	43.0	44.1	34.1	1.0	0	6.0	2.6
6	98.0	10.8	33.5	42.2	2.6	0	0	2.2

Reaction condition; 1st bed: temperature: 300°C, contact time: 177 g.h.mol^{-1}, catalyst: H-ZSM-5 (12.5), 2nd bed: temperature: 175°C, ambient pressure, contact time: 177 g.h.mol^{-1}, catalyst: Ni/SiO_2, feed: 1.575 g.h^{-1} of glycerol at 10 wt.%, 100 ml/min hydrogen.

Table E3 The yield of the glycerol deoxygenation over zeolite H-ZSM-5 and 20 wt.% Ni/Al_2O_3 at contact time = 177 g.h.mol^{-1}

Time on steam	Conversion in 2nd bed		Yield (%)					
(h)	Acrolein	Hydroxy-acetone	1-Propanol	Propional-dehyde	Propanoic acid	Acetalde-hyde	Ethanol	Acetic acid
1	100	100	72.3	6.6	0.5	0	20	0
2	98.9	100	73.8	5.3	0	2.7	13.1	4.2
3	98.8	100	71.5	6.2	1.4	2.7	11.0	6.3
4	99.5	91.3	67.3	7.5	5.3	2.0	7.0	8.9
5	98.7	87.3	69.9	10.7	1.6	3.2	7.5	3.5
6	99.2	80.2	67.2	9.0	3.1	3.3	9.4	3.3

**The conditions are same as Table E2*

Table E4 The yield of the glycerol deoxygenation over zeolite H-ZSM-5 and 20 wt.% Ni/TiO_2 at contact time = 177 g.h.mol^{-1}

Time on steam	Conversion in 2nd bed		Yield (%)					
(h)	Acrolein	Hydroxy-acetone	1-Propanol	Propional-dehyde	Propanoic acid	Acetalde-hyde	Ethanol	Acetic acid
1	98.9	100	68.9	6.4	3.8	1.6	13.4	5.0
2	99.1	89.7	65.6	9.6	5.1	2.4	7.3	8.2
3	99.1	60.6	60.1	13.3	5.9	1.8	3.8	5.9
4	98.8	44.1	52.5	20.9	5.6	1.7	1.4	5.6
5	98.5	48.3	46.7	27.8	4.3	1.7	1.1	4.3
6	98.5	39.7	45.1	30.7	3.0	1.6	1.2	3.0

**The conditions are same as Table E2*

Table E5 The yield of the glycerol deoxygenation over zeolite H-ZSM-5 and 20 wt.% Ni/LDH at contact time = 177 g.h.mol^{-1}

Time on steam	Conversion in 2nd bed		Yield (%)					
(h)	Acrolein	Hydroxy-acetone	1-Propanol	Propional-dehyde	Propanoic acid	Acetalde-hyde	Ethanol	Acetic acid
1	100	100	70.3	9.7	0	2.9	17.1	0
2	99.2	82.0	62.5	16.9	0	6.2	10.2	0
3	98.6	37.2	59.2	19.4	0.3	3.4	4.1	0
4	98.8	51.3	48.3	27.5	3.3	3.1	2.4	4.7
5	98.5	51.3	45.0	26.8	7.0	1.6	1.3	7.4
6	98.4	47.2	40.8	31.7	6.3	1.9	1.2	6.3

**The conditions are same as Table E2*

Table E6 The yield of the glycerol deoxygenation over zeolite H-ZSM-5 and 20 wt.% Ni/MgO at contact time = 177 g.h.mol^{-1}

Time on steam	Conversion in 2nd bed		Yield (%)					
(h)	Acrolein	Hydroxy-acetone	1-Propanol	Propional-dehyde	Propanoic acid	Acetalde-hyde	Ethanol	Acetic acid
1	97.4	100	37.7	38.7	1.5	7.3	12.7	0
2	92.1	75.9	33.7	33.2	6.8	4.6	3.3	7.3
3	78.4	54.5	21.0	33.9	7.8	3.2	1.1	6.6
4	75.2	50.0	19.2	33.6	7.6	3.3	1.0	5.7
5	64.6	38.7	15.1	32.2	4.3	3.4	0.7	3.6
6	55.3	56.7	7.6	29.0	7.6	9.7	0	1.7

**The conditions are same as Table E2*

Table E7 The yield of the glycerol deoxygenation over zeolite H-ZSM-5 and 20 wt.% Ni/C at contact time = 177 g.h.mol^{-1}

Time on steam	Conversion in 2nd bed		Yield (%)					
(h)	Acrolein	Hydroxy-acetone	1-Propanol	Propionaldehyde	Propanoic acid	Acetalde-hyde	Ethanol	Acetic acid
1	92.2	100	0	52.0	21.8	5.7	0	14.3
2	77.0	100	0	45.2	16.4	6.4	0	16.4
3	60.453.1	36.0	0	37.8	10.6	3.1	0	10.6
4	53.0	24.6	0	37.7	4.7	2.5	0	4.7
5	50.1	15.6	0	36.8	3.3	1.8	0	3.3
6	52.0	11.2	0	41.5	0	2.2	0	0

**The conditions are same as Table E2*

E3 : Glycerol deoxygenation over zeolite H-ZSM-5 and 20 wt.% Ni/SiO_2

E3.1 Effect of Contact time

Table E8 Product distribution from the reaction of acrolein from glycerol dehydration over 20 wt.% Ni/SiO_2 catalyst at various contact times.

Contact time ($g.h.mol^{-1}$)	15	29	59	177
Conversion of acrolein (%)	57.7	71.1	97.4	99.4
Yield of product (%)				
1-Propanol	2.0	5.5	41.0	83.7
Propionaldehyde	51.1	43.7	42.5	10.4
Propanoic acid	4.7	22.5	14.0	5.3

Reaction condition; 1st bed: temperature: 300°C, contact time: 177 g.h.mol^{-1}, catalyst: H-ZSM-5 (12.5), 2nd bed: temperature: 175°C, ambient pressure, contact time: 15–177 g.h.mol^{-1}, feed: 1.575 g.h^{-1} of glycerol at 10 wt.%, 100 ml/min hydrogen.

Table E9 The yield of the hydrogenation of acrolein from glecerol dehydration over 20 wt.% Ni/SiO_2 at contact time = 15 g.h.mol^{-1}

Time on steam (h)	Conversion of acrolein (%)	Yield (%)		
		1-Propanol	Propionaldehyde	Propanoic acid
1	63.3	2.4	42.6	5.6
2	57.8	1.7	40.8	3.7
3	51.0	0	38.3	2.5
4	49.0	0	37.0	2.2
5	45.6	0	36.5	0
6	39.4	0	29.6	2.0

Reaction condition; 1st bed: temperature: 300°C, contact time: 177 g.h.mol^{-1}, catalyst: H-ZSM-5 (12.5), 2nd bed: temperature: 175°C, ambient pressure, feed: 1.575 g.h^{-1} of glycerol at 10 wt.%, 100 ml/min hydrogen.

Table E10 The yield of the hydrogenation of acrolein from glecerol dehydration over 20 wt.% Ni/SiO_2 at contact time = 29 g.h.mol^{-1}

Time on steam (h)	Conversion of acrolein (%)	Yield (%)		
		1-Propanol	Propionaldehyde	Propanoic acid
1	87.1	4.7	35.5	29.5
2	71.7	4.4	34.9	18.0
3	70.5	1.7	45.3	9.4
4	69.4	1.9	51.4	2.2
5	68.0	1.3	49.5	3.6
6	68.3	1.4	51.5	1.8

**The conditions are same as Table E9*

Table E11 The yield of the hydrogenation of acrolein from glecerol dehydration over 20 wt.% Ni/SiO_2 at contact time = 59 g.h.mol^{-1}

Time on steam (h)	Conversion of acrolein (%)	Yield (%)		
		1-Propanol	Propionaldehyde	Propanoic acid
1	98.9	40.9	25.1	13.2
2	97.8	32.8	34.0	11.2
3	94.8	19.6	45.8	10.4
4	93.2	14.5	52.1	8.0
5	89.8	9.0	58.7	4.2
6	89.6	9.2	59.6	2.9

**The conditions are same as Table E9*

Table E12 The yield of the hydrogenation of acrolein from glecerol dehydration over 20 wt.% Ni/SiO_2 at contact time = 177 g.h.mol^{-1}

Time on steam (h)	Conversion of acrolein (%)	Yield (%)		
		1-Propanol	Propionaldehyde	Propanoic acid
1	96.9	57.8	8.0	11.6
2	99.4	67.0	8.3	4.3
3	99.4	59.7	18.0	1.8
4	98.8	52.4	24.5	2.0
5	99.0	44.1	34.1	1.0
6	98.0	33.5	42.3	2.6

**The conditions are same as Table E9*

E3.2 Effect of Reaction Temperature

Table E13 Product distribution from the hydrogenation of acrolein from glycerol dehydration over 20 wt.% Ni/SiO_2 at various reaction temperatures.

Reaction Temeprature (°C)	100	120	150	175	200
Contact time (g.h.mol^{-1})	177	177	177	177	177
Conversion of acrolein (%)	98.4	99.9	99.6	98.6	99.2
Yield of product (%)					
1-Propanol	12.6	49.0	40.8	52.4	49.5
Propionaldehyde	56.6	29.0	33.4	22.5	21.9
Propanoic acid	9.5	1.9	5.5	3.9	8.0

Reaction condition; 1st bed: temperature: 300°C, contact time: 177 g.h.mol^{-1}, catalyst: H-ZSM-5 (12.5), 2nd bed: temperature: 175–200°C, ambient pressure, contact time: 177 g.h.mol^{-1}, feed: 1.575 g.h^{-1} of glycerol at 10 wt.%, 100 ml/min hydrogen.

Table E14 The yield of the hydrogenation of acrolein from glecerol dehydration over 20 wt.% Ni/SiO_2 at 100°C

Time on steam (h)	Conversion of acrolein (%)	Yield (%)		
		1-Propanol	Propionaldehyde	Propanoic acid
1	97.9	9.3	56.0	13.0
2	99.0	15.8	51.2	12.2
3	99.2	15.0	55.1	9.3
4	98.3	13.3	58.1	7.3
5	98.2	11.0	61.4	6.2
6	97.8	11.3	57.5	9.4

**The conditions are same as Table E13*

Table E15 The yield of the hydrogenation of acrolein from glecerol dehydration over 20 wt.% Ni/SiO_2 at 120°C

Time on steam (h)	Conversion of acrolein (%)	Yield (%)		
		1-Propanol	Propionaldehyde	Propanoic acid
1	99.7	71.9	5.5	2.3
2	99.8	72.6	6.5	0.8
3	100	55.7	22.7	1.6
4	100	38.0	39.0	2.9
5	100	30.9	45.9	3.2
6	100	24.9	54.2	1.0

**The conditions are same as Table E13*

Table E16 The yield of the hydrogenation of acrolein from glecerol dehydration over 20 wt.% Ni/SiO_2 at 150°C

Time on steam (h)	Conversion of acrolein (%)	Yield (%)		
		1-Propanol	Propionaldehyde	Propanoic acid
1	98.9	68.4	6.2	4.5
2	100	47.3	23.8	8.9
3	98.7	38.1	36.9	4.0
4	100	29.6	42.4	8.0
5	100	30.9	45.6	3.5
6	100	30.8	45.3	3.9

**The conditions are same as Table E13*

Table E17 The yield of the hydrogenation of acrolein from glecerol dehydration over 20 wt.% Ni/SiO_2 at 175°C

Time on steam (h)	Conversion of acrolein (%)	Yield (%)		
		1-Propanol	Propionaldehyde	Propanoic acid
1	96.9	57.8	8.0	11.6
2	99.4	67.0	8.3	4.3
3	99.4	59.7	18.0	1.8
4	98.8	52.4	24.5	2.0
5	99.0	44.1	34.1	1.0
6	98.0	33.5	42.3	2.6

**The conditions are same as Table E13*

Table E18 The yield of the hydrogenation of acrolein from glecerol dehydration over 20 wt.% Ni/SiO_2 at 200°C

Time on steam (h)	Conversion of acrolein (%)	Yield (%)		
		1-Propanol	Propionaldehyde	Propanoic acid
1	96.6	56.7	6.2	14.3
2	100	58.2	13.0	8.7
3	100	51.2	20.7	8.1
4	99.4	46.4	26.6	6.5
5	99.3	44.5	29.0	5.8
6	100	39.8	35.7	4.5

**The conditions are same as Table E13*

Table E19 The yield of the hydrogenation of acrolein from glecerol dehydration over 20 wt.% Ni/SiO_2 at 300°C

Time on steam (h)	Conversion of acrolein (%)	Yield (%)	
		1-Propanol	Propionaldehyde
1	73.1	8.2	8.2
2	94.1	8.4	3.0
3	92.3	4.4	1.4
4	93.2	13.6	4.0
5	96.2	13.8	7.3
6	95.4	14.7	11.4

**The conditions are same as Table E13*

E4 : Glycerol deoxygenation over zeolite H-ZSM-5 and 20 wt.% Ni/Al_2O_3

E4.1 Effect of Contact time

Table E20 Product distribution from the reaction of acrolein from glycerol dehydration over 20 wt.% Ni/Al_2O_3 catalyst at various contact times.

Contact time ($g.h.mol^{-1}$)	15	29	59	177
Conversion of acrolein (%)	65.5	97.5	100	100
Yield of product (%)				
1-Propanol	15.1	51.4	67.3	91.1
Propionaldehyde	44.1	38.5	25.4	8.2
Propanoic acid	6.3	7.6	7.3	0.7

Reaction condition; 1st bed: temperature: 300°C, contact time: 177 $g.h.mol^{-1}$, catalyst: H-ZSM-5 (12.5), 2nd bed: temperature: 175°C, ambient pressure, contact time: 15–177 $g.h.mol^{-1}$, feed: 1.575 $g.h^{-1}$ of glycerol at 10 wt.%, 100 ml/min hydrogen.

Table E21 The yield of the hydrogenation of acrolein from glecerol dehydration over 20 wt.% Ni/Al_2O_3 at contact time = 15 g.h.mol^{-1}

Time on steam (h)	Conversion of acrolein (%)	Yield (%)		
		1-Propanol	Propionaldehyde	Propanoic acid
1	65.5	12.1	35.2	5.1
2	40.6	2.9	26.3	3.3
3	23.7	0	13.9	5.1
4	13.5	0	8.8	2.1
5	14.2	0	8.8	2.6
6	10.0	0	6.6	1.4

Reaction condition; 1st bed: temperature: 300°C, contact time: 177 g.h.mol^{-1}, catalyst: H-ZSM-5 (12.5), 2nd bed: temperature: 175°C, ambient pressure, feed: 1.575 g.h^{-1} of glycerol at 10 wt.%, 100 ml/min hydrogen.

Table E22 The yield of the hydrogenation of acrolein from glecerol dehydration over 20 wt.% Ni/Al_2O_3 at contact time = 29 g.h.mol^{-1}

Time on steam (h)	Conversion of acrolein (%)	Yield (%)		
		1-Propanol	Propionaldehyde	Propanoic acid
1	97.5	41.1	30.8	6.1
2	92.8	26.8	36.6	10.9
3	75.5	9.8	47.3	3.3
4	65.7	4.4	42.5	5.7
5	55.7	2.1	38.9	3.5
6	51.2	1.0	38.2	1.7

**The conditions are same as Table E9*

Table E23 The yield of the hydrogenation of acrolein from glecerol dehydration over 20 wt.% Ni/Al_2O_3 at contact time = 59 g.h.mol^{-1}

Time on steam (h)	Conversion of acrolein (%)	Yield (%)		
		1-Propanol	Propionaldehyde	Propanoic acid
1	100	53.8	20.3	5.8
2	97.4	31.1	38.2	8.7
3	93.2	22.8	41.8	10.0
4	89.4	19.2	44.8	7.5
5	92.1	20.7	48.9	4.1
6	90.9	12.9	56.0	3.9

**The conditions are same as Table E9*

Table E24 The yield of the hydrogenation of acrolein from glecerol dehydration over 20 wt.% Ni/Al_2O_3 at contact time = 177 g.h.mol^{-1}

Time on steam (h)	Conversion of acrolein (%)	Yield (%)		
		1-Propanol	Propionaldehyde	Propanoic acid
1	100	72.9	6.6	0.5
2	98.9	73.8	5.3	0
3	98.8	71.5	6.2	1.4
4	99.5	67.4	7.0	5.3
5	98.7	69.9	7.5	1.6
6	99.1	67.2	9.0	3.1

**The conditions are same as Table E9*

ภาคผนวก ง

สรุปค่าใช้จ่ายการดำเนินโครงการวิจัย

			บันทึกรายการรับ-จ่ายเงิน โครงการวิจัย สัญญาเลขที่ .....2559-01-05-067..... ตั้งแต่วันที่ .....1 ต.ค. 2558..... ถึงวันที่ .....30 ก.ย. 2559.....										
แหล่งทุน: คณะวิทยาศาสตร์													
ชื่อโครงการ : การส่งปฏิวัติชีวภาพเพื่อเปลี่ยนกลีเซอรอลให้เป็นแลคเอสเตอร์													
ชื่อหัวหน้าโครงการ: รศ.ดร.สะวัน สุขน้อย													
ว/ด/ป	รายการ	เลขที่อ้างอิง	รายการรับ - จ่าย			รายรับ	รายจ่าย						รวม
			รับ	จ่าย	คงเหลือ	ดอกเบี้ยรับ	งบบุคลากร	งบดำเนินงาน				งบลงทุน	รายจ่าย
							ค่าจ้างชั่วคราว	ค่าตอบแทน	ค่าใช้สอย	ค่าวัสดุ	ค่าสาธารณูปโภค	ค่าครุภัณฑ์	
	งบประมาณที่ได้รับการอนุมัติ (ตามแผน)												-
	จำนวนเงินที่ได้รับ (งวดที่ 1 = 85%)		255,000.00										
	จำนวนเงินที่ได้รับ (งวดที่ 2 = 15%)		45,000.00										
	จำนวนเงินที่ได้รับ (งวดที่ 3)												
	หัก ค่าใช้จ่าย (ครั้งที่ 1)			183,172.49			60,000.00	-	33,785.00	89,387.49	-	-	183,172.49
	ค่าใช้จ่าย (ครั้งที่ 2)			116,925.68			30,000.00	-	9,941.00	76,984.68	-	-	116,925.68
	งบประมาณคงเหลือ		300,000.00		98.17	0.00							
	รายละเอียดค่าใช้จ่าย												
ครั้งที่ 1													
1 พ.ย. 58	Plug	017/847								120.00			120.00
3 พ.ย. 58	Aluminium Isopropoxide	IV15-110728								1,764.43			1,764.43
4 พ.ย. 58	สายพาน + ปรอท	538/039								170.00			170.00
	Glass blowing									1,000.00			1,000.00
	Nuts									272.00			272.00
9 พ.ย. 58	ICP analysis	0070/00360							2,020.00				2,020.00
26 พ.ย. 58	Nitrogen 99.99%	15001119 RP								856.00			856.00
27 พ.ย. 58	Rotameter	RC5811007								7,811.00			7,811.00
27 พ.ย. 58	Rotameter	RC5811008								7,811.00			7,811.00
	Needle	32859								952.30			952.30
	Vial	32843								2,461.00			2,461.00
18 ธ.ค. 58	Cylinder rental	530891								2,568.00			2,568.00
	Syringe (Gas tight 10mL)	33009								3,745.00			3,745.00
8 ม.ค. 59	Hydrogen 99.99%	16000029 RP								2,033.00			2,033.00
	Xerox									250.00			250.00
19 ม.ค. 59	SS Pellet Mold	IV590100034								2,140.00			2,140.00
22 ม.ค. 59	VGA Card, Harddisk	SR5901/0000034								4,280.00			4,280.00
22 ม.ค. 59	UPS, Plug Surge	2635127/255160								2,347.00			2,347.00
2 ก.พ. 59	MAS NMR	109/123							9,600.00				9,600.00
	Syringe (Gas tight 10mL)	33285								3,745.00			3,745.00
	Hose									130.00			130.00
10 ก.พ. 59	Thermocouple SK11 2.3x500mm	SI2559/0139								3,852.00			3,852.00
10 ก.พ. 59	Thermocouple SK11 1x300mm	SI2559/0137								2,407.50			2,407.50
10 ก.พ. 59	Heating Tape 150W	SI2559/0138								1,926.00			1,926.00
8 มี.ค. 59	Aluminium foil									130.00			130.00
	Balloon	3382								60.00			60.00
	Syringe (Plastic 50CC)									60.00			60.00
	Cable									489.00			489.00
	Glass Cutter									240.00			240.00
	Glass bead 500-700micron 500g	IV16-030567								7,420.99			7,420.99
15 มี.ค. 59	XRD	109/400							1,450.00				1,450.00
15 มี.ค. 59	XRD	109/402							2,900.00				2,900.00
20 มี.ค. 59	XRD	112/213							850.00				850.00
28 มี.ค. 59	Fitting	2664/133199								1,929.42			1,929.42
	Washing Liquid									26.00			26.00
29 มี.ค. 59	Glass Blowing									400.00			400.00
31 มี.ค. 59	BET	18589/22							2,000.00				2,000.00
31 มี.ค. 59	Salary						15,000.00						15,000.00
7 เม.ย. 59	BET	2960/10							5,000.00				5,000.00
10 เม.ย. 59	Quartz Tube	PN590035								2,140.00			2,140.00
11 เม.ย. 59	XRD	118/100							4,125.00				4,125.00
19 เม.ย. 59	Xerox	27/1307								75.00			75.00
19 เม.ย. 59	ICP analysis	0557/00655							3,340.00				3,340.00
	Calcium oxalate	IV16-040828								3,217.49			3,217.49
26 เม.ย. 59	AC Adapter	OCT5904000070								802.50			802.50
28 เม.ย. 59	Nitrogen 99.99%	16000539 RP								4,280.00			4,280.00
30 เม.ย. 59	Salary						15,000.00						15,000.00
13 พ.ค. 59	Air-zero Gas	16000612 RP								5,136.00			5,136.00
18 พ.ค. 59	Co complex	IV605488								2,885.36			2,885.36
	Xerox	248/12361								1,440.00			1,440.00
	Washing Liquid									58.00			58.00
	Aluminium Foil									65.00			65.00
	Balloon	03408	-	-	-	-				97.00			97.00
	Cr complex	IV16061179								5,189.50			5,189.50
	Bottle									250.00			250.00
	Cu Tube									195.00			195.00
31 พ.ค. 59	Salary						15,000.00						15,000.00
7 มิ.ย. 59	PP Box									160.00			160.00
28 มิ.ย. 59	Refrigerator repair	035/1736							2,500.00				2,500.00
30 มิ.ย. 59	Salary						15,000.00						15,000.00
	รวมครั้งที่ 1		-	-	-	-	60,000.00	-	33,785.00	89,387.49	-	-	183,172.49

บันทึกรายการรับ-จ่ายเงิน โครงการวิจัย สัญญาเลขที่ .....2559-01-05-067..... ตั้งแต่วันที่ .....1 ส.ค. 2558..... ถึงวันที่ .....30 ก.ย. 2559.....

แหล่งทุน: คณะวิทยาศาสตร์

ชื่อโครงการ : การส่งปฏิกิริยาเพื่อเปลี่ยนคลีเซอรอลให้เป็นแอลกอฮอล์

ชื่อหัวหน้าโครงการ: รศ.ดร.สะวัน สุขน้อย

ว/ด/ป	รายการ	เลขที่อ้างอิง	รายการรับ - จ่าย			รายรับ	รายจ่าย						รวม
			รับ	จ่าย	คงเหลือ	ดอกเบี้ยรับ	งบบุคลากร	งบดำเนินงาน				งบลงทุน	รายจ่าย
							ค่าจ้างชั่วคราว	ค่าตอบแทน	ค่าใช้สอย	ค่าวัสดุ	ค่าสาธารณูปโภค	ค่าครุภัณฑ์	
ครั้งที่ 2	**(After 14/07/59)**												
15 ก.ค. 59	Xerox	247/12322							616.00				616.00
15 ก.ค. 59	Xerox	247/12321							1,000.00				1,000.00
	Beaker low form 1000 & 2000mL	SPCIRG16070057								4,700.08			4,700.08
	Volumetric Flasks	SPCIRG16070055								4,250.04			4,250.04
22 ก.ค. 59	Printer Toner	0002407161008463								3,980.00			3,980.00
	Flask round bottom 500ml	SPCIRG16070060								4,989.84			4,989.84
28 ก.ค. 59	Glass Blowing									600.00			600.00
31 ก.ค. 59	Salary						15,000.00						15,000.00
2 ส.ค. 59	Quartz Wool	5712070								3,210.00			3,210.00
	Graphite Liners	34693								4,494.00			4,494.00
	Septa BTO	34694								3,477.50			3,477.50
	1MR-GT	34687								3,210.00			3,210.00
	Quartz Tube	PN590092								8,003.60			8,003.60
	Union	IV.5908023								2,420.34			2,420.34
5 ส.ค. 59	Zip Bag									180.00			180.00
5 ส.ค. 59	Solid state relay	SR59/3896								2,696.40			2,696.40
5 ส.ค. 59	Heating Tape	SR59/3894								4,078.84			4,078.84
5 ส.ค. 59	XRD	0551/00174							2,580.00				2,580.00
11 ส.ค. 59	Air-zero gas	16000997 RP								9,202.00			9,202.00
	Hotplate repair	00017478							3,745.00				3,745.00
	Triphenyl phosephine	IV16-08298								5,303.67			5,303.67
	Octane	IV16-080692								3,051.43			3,051.43
	Tetraamine platinum nitrate	IV16-08653								4,408.47			4,408.47
	Tetraamine platinum nitrate	IV16-08655								4,408.47			4,408.47
	SS Ring	0432								70.00			70.00
	Xerox									250.00			250.00
	Report preparation								2,000.00				2,000.00
31 ส.ค. 59	Salary						15,000.00						15,000.00
	รวมครั้งที่ 2		-	-	-	-	30,000.00	-	9,941.00	76,984.68	-	-	116,925.68

ลงชื่อหัวหน้าโครงการ .....

วันที่ .....

ประวัตินักวิจัย

หัวหน้าโครงการวิจัย

1. ชื่อ - นามสกุล (ภาษาไทย)

   รศ.ดร.ตะวัน สุขน้อย

2. ชื่อ - นามสกุล (ภาษาอังกฤษ)

   Assoc.Prof.Tawan Sooknoi

3. ตำแหน่งปัจจุบัน

   รองศาสตราจารย์

4. หน่วยงานและสถานที่อยู่ที่ติดต่อ

   ภาควิชาเคมี คณะวิทยาศาสตร์ สถาบันเทคโนโลยีพระจอมเกล้าเจ้าคุณทหารลาดกระบัง

   1 ซ.ฉลองกรุง1 แขวงลาดกระบัง เขตลาดกระบัง กรุงเทพ 10520

   โทรศัพท์ 02 329 8400-11 ต่อ 6250 โทรสาร 02 329 8428 โทรศัพท์มือถือ 081 929 8288

   อีเมล์ kstawan@gmail.com

5. ประวัติการศึกษา

   2530-2534 วท.บ. สถาบันเทคโนโลยีพระจอมเกล้าเจ้าคุณทหารลาดกระบัง

   2535-2536 M.Sc. University of Manchester Institute of Science and Technology, UK

   2536-2537 Ph.D. University of Manchester Institute of Science and Technology, UK

6. สาขาวิชาการที่มีความชำนาญพิเศษ (แตกต่างจากวุฒิการศึกษา) ระบุสาขาวิชาการ

   Applied Chemistry, Zeolite and Heterogeneous Catalysis

7. ประสบการณ์ที่เกี่ยวข้องกับการบริหารงานวิจัยทั้งภายในและภายนอกประเทศ

ปี 2556

(i) Decarbonylation / Decarboxylation of fatty acid to produce renewable long chain α-olefin, ทุนวิจัยองค์ความรู้ใหม่ที่เป็นพื้นฐานต่อการพัฒนา (วุฒิเมธีวิจัย สกว.), สำนักงานกองทุนสนับสนุนการวิจัย (3 ปี).

(ii) Swift response catalytic testing system for innovative approach, Research & Development Grant, SCG Chemicals Co.,Ltd. (1 year).

(iii) Glycerol conversion to C3 alcohols, Research & Development Grant, PTT Public Co.,Ltd. (1.2 year).

ปี 2554

(i) Controlled deoxygenation of cellulose to chemicals and hydrocarbon feedstocks, Research & Development Grant, PTT Public Co., Ltd. (1.5 year).

(ii) Synthesis of Zeolite A Nanoparticles, Research & Development Grant, PQ Chemicals Co., Ltd. (1 year).

(iii) Catalytic Conversion of Glycerol to C3 Petrochemicals, Research & Development Grant, PTT Public Co., Ltd. (1 year).

(iv) Preparation of tunable PS/PMMA block copolymer, Research & Development Grant, IRPC Co., Ltd. (1.5 year).

งานวิจัยที่ทำเสร็จแล้ว :

(i) Role of Keto Intermediates in the Hydrodeoxygenation of Phenol over Pd on Oxophilic Supports, Priscilla M. de Souza, Raimundo C. Rabelo-Neto, Luiz E. P. Borges, Gary Jacobs, Burtron H. Davis, **Tawan Sooknoi,** Daniel E. Resasco, and Fabio B. Noronha, *ACS Catalysis*, 5 (2015) pp 1318–1329.

(ii) Oxidation of Tetrahydrofuran to Butyrolactone Catalyzed by Iron-containing Clay, Artit Ausavasukhi and **Tawan Sooknoi**, *Green Chemistry*, 17 (2015) 435-441.

(iii) Catalytic Activity Enhancement by Thermal Treatment and Reswelling Process of Natural Containing Fe-Clay for Fenton Oxidation, Artit Ausavasukhi, **Tawan Sooknoi**, *Journal of Colloid and Interface Science*, **436** (2014) 37–40.

(iv) Selective, Conversion of m-Cresol to Toluene over, Bi,etallic Ni-Fe Catalysts, Lei Nie, Priscilla M. de Souza, Fabio B. Noronha, Wei An,**Tawan Sooknoi**, Daniel E. Resasco, *Journal of Molecular Catalysis A: Chemica*l, **388–389** (2014) 47–55.

(v) Hydrophobic Zeolite-Filled Polymeric Films with High Ethylene Permselectivity for Fresh Produce Packaging Applications, Fuongfuchat, A., Sirikittikul, D., Booncharoen, W., Raksa, P., Ritvirulh, C., **Sooknoi, T**. *Packaging Technology and Science, Volume 27, Issue 10, pages 763–773, October 2014*.

(vi) Tunable Activity of [Ga]HZSM-5 with H2 Treatment: Ethane Dehydrogenation, Artit Ausavasukhi, **Tawan Sooknoi**, *Catalysis Communications*, 45 (2014) 63–68.

(vii) Ketonization of carboxylic Acids: Mechanisms, Catalysts, and Applications in Bio-oil Upgrading, Tu N Pham, **Tawan Sooknoi** , Steven Crossley, Daniel E. Resasco, *ACS Catalysis*, 3 (2013), 2456–2473.

(viii) Aqueous-phase ketonization of acetic acid over Ru/TiO_2/carbon catalysts, Tu Nguyet Pham, Dachuan Shi, **Tawan Sooknoi**, Daniel E. Resasco, *Journal of Catalysis*, 295 (2012), 169-178.

(ix) Aromatization of Cyclopentane Over ZSM-5 Catalysts: A Proposal of Reaction Pathway, N. Peamaroon, **T. Sooknoi**, *Petroleum Science and Technology*, Volume 30(16) (2012), 1647-1655.

(x) Hydrodeoxygenation of m-cresol over gallium-modified beta zeolite catalysts, Artit Ausavasukhi, Yi Huang, Anh T. To, **Tawan Sooknoi**, Daniel E. Resasco, *Journal of Catalysis*, 290 (2012), 90-100.

(xi) Direct conversion of glycerol to acrylic acid via integrated dehydration-oxidation bed system, Ayut Witsuthammakul and **Tawan Sooknoi**, *Applied Catalysis A - General*, 413-414 (2012) 109-116.

(xii) Effect of extra-framework cesium on the deoxygenation of methylester over CsNaX zeolites, Tanate Danuthai, **Tawan Sooknoi**, Siriporn Jongpatiwut, Thirasak Rirksomboon, Somchai Osuwan, Daniel E. Resasco, *Applied Catalysis A - General*, 409-410 (2011) 74-81.

(xiii) Selective ethylene-permeable zeolite composite double-layered film for novel modified atmosphere packaging, P. Monprasit, C. Ritvirulh, **T. Sooknoi,** S. Rukchonlatee, A. Fuongfuchat, D. Sirikittikul, *Polymer Engineering & Science*, 51(7) (2011) 1264-1272.

(xiv) Conversion of Furfural and 2-Methylpentanal on Pd/SiO2 and Pd-Cu/SiO2 Catalysts, Surapas Sitthisa, Trung Pham, Teerawit Prasomsri, **Tawan Sooknoi**, Richard G. Mallinson, Daniel E. Resasco, *Journal of Catalysis*, 280 (2011) 17-27**.**

(xv) Kinetics and Mechanism of Hydrogenation of Furfural on Cu/SiO2 Catalysts, Surapas Sitthisa, **Tawan Sooknoi**, Yuguang Ma, Perla B. Balbuena, Daniel E. Resasco, *Journal of Catalysis*, 277 (2011) 1-13

ผลงานวิจัยจดทะเบียนสิทธิบัตร 5 ปีย้อนหลัง

(i) United State Patent, US 8,697,777 B2, *Master Batch for preparing plastic films with high etylene permselectivity and the plastic films produced therefrom*, April 15th, 2014.

(ii) เลขที่คำขอจดทะเบียน 1301007386
กระบวนการเปลี่ยนชีวมวลลิกโนเซลลูโลสเป็นเชื้อเพลิงและสารประกอบเคมีพื้นฐานที่มีออกซิเจนต่ำ 26 ธันวาคม 2556

(iii)

เลขที่คำขอจดทะเบียน 1101000205 การผลิตไฮโดรคาร์บอนสายยาวจากปฏิกิริยาดีคาร์บอกซิเลชันของกรดปาล์มมิติกโดยใช้โลหะออกไซด์เป็นตัวเร่งปฏิกิริยา, 15 กุมภาพันธ์ 2554

(iv)

เลขที่คำขอจดทะเบียน 6284 อนุสิทธิบัตร ตัวตรวจวัดแก๊สชนิดฟิล์มบางโลหะออกไซด์ที่เคลือบด้วยแผ่นเยื่อซิลิกาไลต์-1ชนิดเด่นระนาบ 010, 2554

งานวิจัยที่กำลังทำ :

Decarbonylation / Decarboxylation of fatty acid to produce renewable long chain α-olefin, ทุนวิจัยองค์ความรู้ใหม่ที่เป็นพื้นฐานต่อการพัฒนา (วุฒิเมธีวิจัย สกว.), สำนักงานกองทุนสนับสนุนการวิจัย (3 ปี) การวิจัยลุล่วงแล้วประมาณ 60%

ผู้ร่วมวิจัย

1. ชื่อ - นามสกุล (ภาษาไทย)
   ดร. ณัฐธิดา นุ่มวงศ์

2. ชื่อ - นามสกุล (ภาษาอังกฤษ)
   Natthida Numwong

3. ตำแหน่งปัจจุบัน
   อาจารย์

4. หน่วยงานและสถานที่อยู่ที่ติดต่อได้สะดวก
   ภาควิชาเคมี คณะวิทยาศาสตร์ สถาบันเทคโนโลยีพระจอมเกล้าเจ้าคุณทหารลาดกระบัง

   1 ซ.ฉลองกรุง1 แขวงลาดกระบัง เขตลาดกระบัง กรุงเทพ 10520

   โทรศัพท์ 02-329 8400-11 ต่อ 344 โทรสาร 02-329 8428

   E-mail: knnatthi@kmitl.ac.th

5. ประวัติการศึกษา
   2550 – วท.บ. เทคโนโลยีปิโตรเคมี (เกียรตินิยมอันดับ 1)
   สถาบันเทคโนโลยีพระจอมเกล้าเจ้าคุณทหารลาดกระบัง

   2556 – ปร.ด. เทคโนโลยีปิโตรเคมี วิทยาลัยปิโตรเลียมและปิโตรเคมี
   จุฬาลงกรณ์มหาวิทยาลัย

6. สาขาวิชาการที่มีความชำนาญพิเศษ
   สาขาวิศวกรรมศาสตร์และอุตสาหกรรมวิจัย

7. ประสบการณ์งานวิจัยที่เกี่ยวข้อง
   7.1 หัวหน้าโครงการวิจัย : Deoxygenation of glycerol to C3 alcohols

   แหล่งทุน: งบประมาณเงินรายได้ คณะวิทยาศาสตร์ ประจำปี 2558
   ประเภทส่งเสริมนักวิจัย

   งานวิจัยลุล่วงร้อยละ: 50

   7.2 ผู้ร่วมวิจัย (Postdoctoral Fellow): Hydrodeoxygenation of vegetable oil for renewable diesel production

แหล่งทุน: ทุนนักวิจัยรุ่นเยาว์ สถานเอกอัครราชทูตฝรั่งเศสประจำประเทศไทย ประจำปี 2557

สถานที่ทำวิจัย: IRCELyon ประเทศฝรั่งเศส

7.3 ผู้ร่วมวิจัย (Ph.D. student): Partial hydrogenation of poly-unsaturated FAMEs for biodiesel upgrading

แหล่งทุน: ทุนปริญญาเอก จุฬาดุษฎีภิพรรธน์ ประจำปี 2551

สถานที่ทำวิจัย: AIST ประเทศญี่ปุ่น

ผลงานวิจัยในระดับนานาชาติ

(i) **Numwong N.**, Luengnaruemitchai A., Chollacoop N., and Yoshimura Y., Effect of SiO_2 Pore Size on Partial Hydrogenation of Rapeseed Oil-Derived FAMEs. *Applied Catalysis A:General*, 441–442 (2012) 72–78

(ii) **Numwong N.**, Luengnaruemitchai A., Chollacoop N., Yoshimura Y., Partial Hydrogenation of Polyunsaturated Fatty Acid Methyl Esters over Pd/Activated Carbon: Effect of Type of Reactor. *Chemical Engineering Journal*, 210 (2012) 173–181

(iii) **Numwong N.**, Luengnaruemitchai A., Chollacoop N., and Yoshimura Y., Effect of Support Acidic Properties on Sulfur Tolerance of Pd Catalysts for Partial Hydrogenation of Rapeseed Oil-Derived FAME. *Journal of the American Oil Chemists' Society*, 89 (2012) 2117–2120

(iv) **Numwong N.**, Luengnaruemitchai A., Chollacoop N., and Yoshimura Y., Effect of Metal Type on Partial Hydrogenation of Rapeseed Oil-Derived FAME. *Journal of the American Oil Chemists' Society*, 90 (2013) 1431–1438